

1 Genome assembly and isoform analysis of a highly
2 heterozygous New Zealand fisheries species, the tarakihi
3 (*Nemadactylus macropterus*).

4 Yvan Papa^a, Maren Wellenreuther^{b,c}, Mark A. Morrison^d, Peter A. Ritchie^{a*}

5 ^a*School of Biological Sciences, Victoria University of Wellington, PO Box 600, Wellington 6140,*
6 *New Zealand;* ^b*Seafood Production Group, The New Zealand Institute for Plant and Food*
7 *Research Limited, Box 5114, Port Nelson, Nelson 7043, New Zealand;* ^c*School of Biological*
8 *Sciences, The University of Auckland, Private Bag 92019, Auckland 1142, New Zealand;*
9 ^d*National Institute of Water and Atmospheric Research, PO Box 109 695, Newmarket,*
10 *Auckland, New Zealand;*

11 *Corresponding author. (Email: peter.ritchie@vuw.ac.nz Address: School of Biological
12 Sciences, Victoria University of Wellington, PO Box 600, Wellington 6140, New Zealand)

13 Running head: Genome assembly of tarakihi

14 **Abstract**

15 Although being some of the most valuable and heavily exploited wild organisms, few fisheries
16 species have been studied at the whole-genome level. This is especially the case in New
17 Zealand, where genomics resources are urgently needed to assist fisheries management
18 attains its sustainability goals. Here we generated 55 Gb of short Illumina reads (92×
19 coverage) and 73 Gb of long Nanopore reads (122×) to produce the first genome assembly of
20 the marine teleost tarakihi (*Nemadactylus macropterus*), a highly valuable fisheries species in
21 New Zealand. An additional 300 Mb of Iso-Seq RNA reads were obtained from four tissue
22 types of another specimen to assist in gene annotation. The final genome assembly was 568
23 Mb long and consisted of 1,214 scaffolds with an N50 of 3.37 Mb. The genome completeness

24 was high, with 97.8% of complete Actinopterygii BUSCOs. Heterozygosity values estimated
25 through k-mer counting (1.00%) and bi-allelic SNPs (0.64%) were high compared to the same
26 values reported for other fishes. Repetitive elements covered 30.45% of the genome and
27 20,169 protein-coding genes were annotated. Iso-Seq analysis recovered 91,313 unique
28 transcripts (isoforms) from 15,515 genes (mean ratio of 5.89 transcripts per gene), and the
29 most common alternative splicing event was intron retention. This highly contiguous genome
30 assembly along with the isoform-resolved transcriptome will provide a useful resource to
31 assist the study of population genomics, as well as comparative eco-evolutionary studies in
32 other teleost and related organisms.

33 **Keywords:** Fish, genomics, Iso-Seq, marine, teleost, transcriptome

34 **1. Introduction**

35 The tarakihi or jackass morwong (*Nemadactylus macropterus*, Centrarchiformes: Cirrhitioidei,
36 NCBI Taxon ID: 76931) is a species of demersal marine teleost fish that is widely distributed
37 around all inshore areas of New Zealand and along the southern coasts of Australia. It is
38 distinguishable from other New Zealand “morwongs” by the black saddle across its nape
39 (Roberts et al., 2015) and displays a single elongated pectoral fin ray that is characteristic of
40 *Nemadactylus* species (Ludt et al., 2019). The species and its genus have been recently moved
41 from the Cheilodactylidae to the Latridae following extensive revision of the taxonomy of
42 both families, which until then was poorly understood (Kimura et al., 2018; Ludt et al., 2019).
43 Tarakihi is an important commercial and recreational inshore fishery, especially in New
44 Zealand, where more than 5,000 tonnes are harvested every year (Fisheries New Zealand,
45 2018). Like many other fisheries species, tarakihi stocks have been heavily fished over the
46 past century. As a result, the spawning biomass is now concerningly depleted to numbers
47 below the fisheries management soft limit of 20% on the east coast of New Zealand, where
48 fishing effort is highest (Langley, 2018). Low effective population size and spawning biomass
49 are of concern for the long-term sustainability of this species, particularly with added and
50 increasing environmental pressures due to global warming. Climate change is already

51 impacting marine ecosystems and is expected to affect the distribution and productivity of
52 many fisheries species (Babcock et al., 2019; Burrows et al., 2011; Ramos et al., 2018).

53 The application of genome-wide markers for tarakihi fisheries management has been limited
54 by the lack of a reference genome. Consequently, the first step in developing new genomic
55 resources for this species is to assemble a high-quality reference genome that can be used to
56 develop high-resolution markers for determining the genetic stock structure. This would offer
57 the potential to estimate gene flow levels and detect adaptive genetic variation.
58 Incorporating adaptive genetic variation, along with neutral variation, will greatly improve
59 how the genetic data can be used for fisheries management (Benestan, 2019; Bernatchez et
60 al., 2017; Papa, Oosting, et al., 2021; Thomson et al., 2021). While the neutral markers can
61 detect reproductively isolated stocks, the adaptive loci can detect differentiation in
62 reproductive success of migrant fish moving to locally adapted stocks. Using high-resolution
63 markers sets for both neutral and adaptive variation has the potential to revolutionize the
64 way genetic markers are used to define fisheries stocks.

65 As DNA sequencing technology is rapidly changing and improving, a range of sequencing data
66 types has been used to produce genome assemblies, thus providing a range of genome
67 qualities, contiguity, and completeness depending on the available technology and
68 investment level. While short-read Illumina sequencing produces highly accurate reads, their
69 short length (usually less than 200 bp) makes them computationally difficult to assemble. This
70 is particularly problematic for regions that span highly repetitive segments of the genome.
71 Complex genomes often result in highly fragmented assemblies (Koren et al., 2012; Rice &
72 Green, 2019). The development of less accurate but long-read sequencing technologies from
73 Oxford Nanopore and Pacific Biosciences (PacBio) has improved the assembly process by
74 combining them with short-read data to create “hybrid”, more contiguous genome
75 assemblies (Austin et al., 2017; Dhar et al., 2019; Jiang et al., 2019; Tan et al., 2018; Wiley &
76 Miller, 2020; Zimin, Puiu, et al., 2017; Zimin, Stevens, et al., 2017).

77 The rapid improvements in sequencing technologies have also improved the ability to collect
78 RNA sequence (RNA-seq) data. Short read RNA-seq data has been used to assist in genome
79 annotation by first assembling a transcriptome and mapping it to the orthologous sequences
80 to find protein-coding genes. A downside of this short read length (c. 100–150 bp) is that it is
81 difficult or impossible to detect and characterize alternative isoforms of the coding
82 sequences, while alternative splicing is known to occur in the vast majority of multi-exon
83 genes (Hardwick et al., 2019). The circular consensus sequencing (CCS) PacBio technology
84 produces reads that are both thousands of bp long and highly accurate (as opposed to the
85 Nanopore and PacBio continuous long reads mentioned above). CCS long-read DNA
86 sequencing can be applied to DNA (i.e. High fidelity, or HiFi reads) and RNA (i.e. isoform
87 sequencing, or Iso-Seq). By capturing the entire sequence length of RNA molecules, Iso-Seq
88 allows for the sequencing of complete, uninterrupted mRNAs, which enables the accurate
89 characterization of isoforms (An et al., 2018; Byrne et al., 2019; Y. Gao et al., 2019; Hoang &
90 Henry, 2021). Iso-Seq has been used to detect and characterize for the first time alternate
91 splicing in the transcriptomes of several organisms, like the human (*Homo sapiens*) (Kuo et
92 al., 2020), the chicken (*Gallus gallus*) (Kuo et al., 2017), or the goldfish (*Carassius auratus*
93 *auratus*) (Gan et al., 2021). Iso-seq is now also used to annotate *de novo* genome assemblies
94 of non-model organisms, like the cave nectar bat (*Eonycteris spelaea*) (Wen et al., 2018), the
95 pharaoh ant (*Monomorium pharaonis*) (Q. Gao et al., 2020), the red-eared slider turtle
96 (*Trachemys scripta elegans*) (Simison et al., 2020), or the sponge gourd (*Luffa* spp.)
97 (Pootakham et al., 2020), allowing for the characterization of both gene functions and
98 alternative splicing patterns.

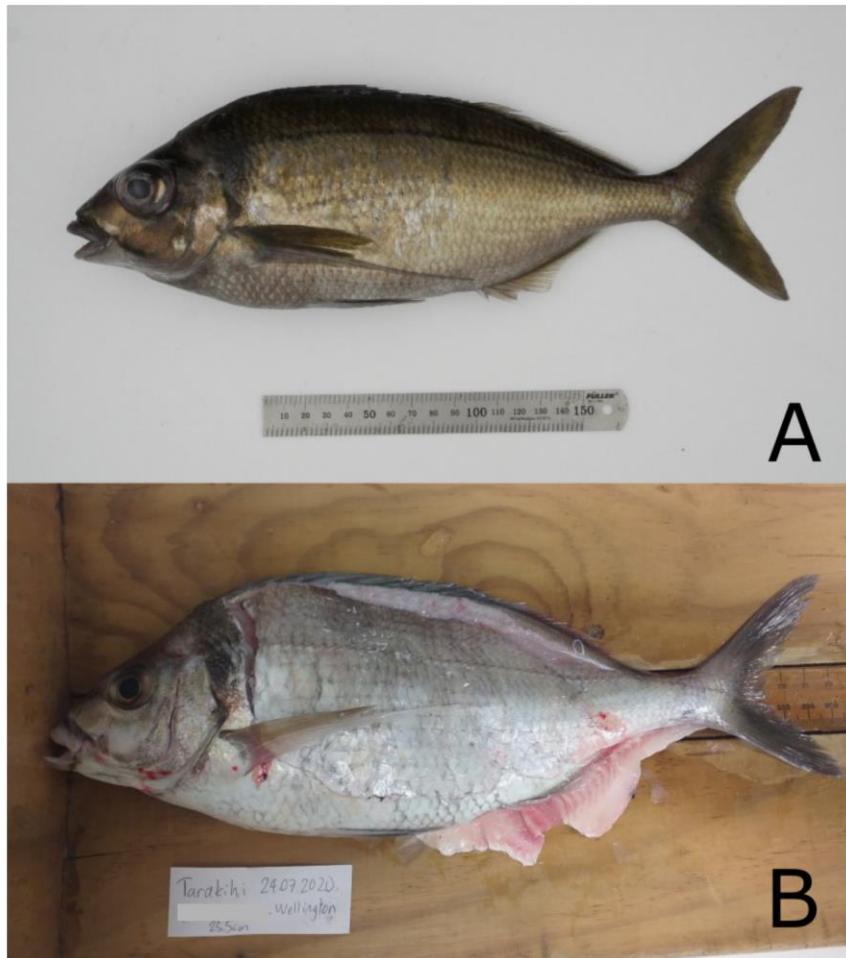
99 The main goal of this study was to complete the first tarakihi genome assembly. This was
100 achieved by using a combination of short-read Illumina and long-read Nanopore sequencing
101 data. Four assembly pipelines were compared, three of which used algorithms implemented
102 in MaSuRCA for hybrid assembly, and a fourth pipeline based on a trial run of low-coverage
103 DNA sequence reads (4 Gb) generated using the PacBio HiFi platform. Iso-Seq data was used
104 to assist with gene annotation and the identification of gene isoforms.

105 **2. Materials and Methods**

106 2.1 Tissue collection and nucleotide extraction

107 Tissues for Illumina and Nanopore sequencing were collected from a freshly vouchered *N.*
108 *macropterus* specimen (standard length: 285 mm, weight: 460 g) identified as male by
109 observation of the gonads. The specimen was a captive-bred from Plant and Food Research,
110 Nelson, New Zealand (Figure 1A) and is thereby referred to as TARdn1 (for “tarakihi *de novo*”).
111 A caudal fin clip and a heart piece were stored in 96% EtOH, and a kidney piece was stored in
112 DESS (20% DMSO, 0.25 M EDTA, NaCl saturated solution). Total genomic DNA was extracted
113 from these tissues using a high-salt extraction protocol adapted from Aljanabi & Martinez
114 (1997) that included an RNase treatment and then suspended in Tris-EDTA buffer (10 mM
115 Tris-HCl pH 8.0, 1 mM EDTA). The integrity of DNA fragments was assessed by gel
116 electrophoresis in 1% agarose. The purity and quantity of DNA (concentration > 200 ng/μl,
117 A260/280 ≈ 1.8, A60/230 ≈ 2, total weight > 20 μg) were estimated with CLARIOstar
118 spectrometer (BMG Labtech). Purified DNA samples were sent to Annoroad Gene Technology
119 Co. Ltd. (Beijing, China) and NextOmics Biosciences Co., Ltd. (Wuhan, China) for Illumina and
120 Nanopore library preparation and sequencing.

121 Tissues for HiFi sequencing and Iso-Seq were obtained from a wild specimen captured by a
122 recreational fisherman at Kau Bay, in the Wellington harbour (New Zealand), thereby referred
123 to as TARdn2 (Figure 1B). The specimen was collected for tissue sampling after being filleted
124 by the fisherman. It had a standard length of 255 mm and was identified as male by
125 observation of the gonads. Tissues were collected a few hours after capture and flash-frozen
126 in liquid nitrogen. Five pieces of tissues were sent to BGI Tech Solutions Co., Ltd. (Hong Kong,
127 China): one tissue (heart) for DNA extraction and HiFi sequencing and four tissues (liver, white
128 muscle, brain, and spleen) for RNA extraction and Iso-Seq. DNA and RNA were extracted by
129 BGI using a phenol-chloroform method.



130

131 Figure 1. Tarakihi specimens used in this study. (A) TARdn1: captive bred specimen used for
132 Illumina and Nanopore sequencing. (B) TARdn2: wild-caught specimen used for HiFi
133 sequencing and Iso-Seq.

134 2.2 Genome size estimation pre-sequencing

135 To estimate the size of the *N. macropterus* genome and ensure there was a sufficient amount
136 of DNA sequencing for adequate coverage, genome information from closely related species
137 was assessed. As of October 2018, only two other Centrarchiformes genome assemblies were
138 deposited in NCBI at the scaffold level (accession numbers: GCA_002120245.1 (Murray cod,
139 *Maccullochella peelii*), and GCA_003416845.1 (barred knifejaw, *Oplegnathus fasciatus*),
140 which had genome lengths of 633.24 and 766.3 Mb. Moreover, the species closest to *N.*
141 *macropterus* for which genome size was estimated on the Animal Genome Size Database
142 (<http://www.genomesize.com>) was the red morwong *Cheilodactylus fuscus*, with a C-value of
143 0.72, or approximately 700 Mb. The genome size of *N. macropterus* was thus estimated to be

144 about 700 Mb. The quantity of Illumina and Nanopore bases to be sequenced was tuned for
145 a deep 85× Illumina coverage (c. 60 Gb) and 140× Nanopore coverage (c. 100 Gb), following
146 sequencing provider recommendations.

147 2.3 Library preparations and sequencing

148 Library preparations, sequencing, and the first filtering step (except for Nanopore reads) were
149 performed by the sequencing providers. For Illumina reads, DNA samples were sheared with
150 Bioruptor® Pico system (Diagenode) for a fragment insert size of 350+/-50 bp, and a PCR-free
151 library was obtained with NEBNext® Ultra™ II DNA Library Prep Kit for Illumina (New England
152 Biolabs). Approximately 200 million of 150 bases pair-end reads were generated using the
153 HiSeq X System (Illumina). Raw Illumina reads were filtered by discarding read pairs if (1) one
154 read contained some adapter contamination for more than five nucleotides, (2) more than
155 10% of bases were uncertain in either one read, or (3) the proportion of bases with Quality
156 Value ≤ 19 was over 50% in either one read. For Nanopore library preparation, large size DNA
157 fragments were selected by automated gel electrophoresis with BluePippin (Sage Science)
158 followed by enrichment and purification using beads. Fragmented DNA was then end-
159 repaired, A-tailed, and purified, and adapter ligation was done using the Ligation Sequencing
160 Kit 1D 108 (Oxford Nanopore Technologies). The resulting DNA library of 20–40 Kb fragments
161 was then loaded into two flow cells for real-time single-molecule sequencing on PromethION
162 (Oxford Nanopore Technologies). Reads were base-called from their raw FAST5 files using
163 Albacore 2.0.1 (<https://community.nanoporetech.com>). HiFi library was prepped with
164 SMRTbell® Express Template Prep Kit 2.0 (Pacific Biosciences) and CCS was performed on one-
165 third of an SMRT Cell 8M with a PacBio Sequel II sequencer. ZMWs were filtered to retain a
166 minimum of three passes and a predicted quality value (RQ) of 99. Four Iso-Seq libraries of 0–
167 5 kb insert sizes (one per tissue) were generated using the SMRTbell® Express Template Prep
168 Kit 2.0. The multiplexed libraries were sequenced on one SMRT Cell 8M with a PacBio Sequel
169 II sequencer, resulting in 3.6 million polymerase reads from which sub-reads were extracted.

170 2.4 Illumina reads: Quality and contamination filtering

171 Primary quality filtering resulted in 405.2 million Illumina pair-end reads (60.78 Gb). Quality
172 metrics of these filtered reads were visualized with FastQC v0.11.7 (Andrews, 2018) before
173 proceeding to the next steps. Kraken v2.0.7-beta (Wood et al., 2019) was used to detect and
174 filter contamination from archaea, bacteria, viral, and human sequences based on the
175 MiniKraken2 v2 8GB database (Wood, 2019). The 9.25% of reads that were classified as
176 contaminants were discarded, leading to 367.8 million non-contaminated reads (55.16 Gb)
177 (Table 1).

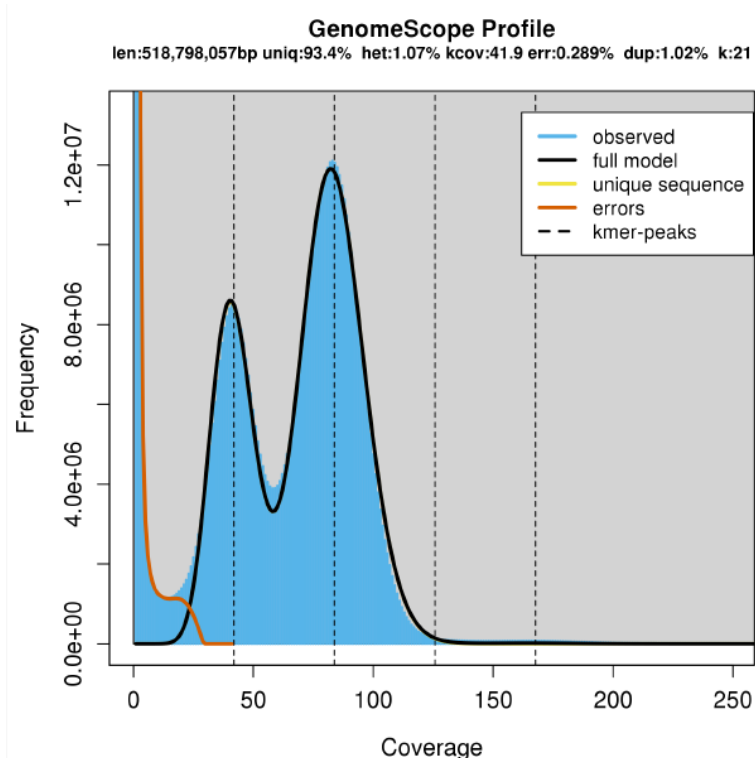
178 2.5 Illumina reads: Mitogenome assembly and exclusion

179 Illumina reads filtered for quality and contamination were mapped against the Peruvian
180 morwong (*Cheilodactylus variegatus*) complete mitochondrial sequence retrieved from
181 Genbank (accession number: KP704218.1) with Geneious v11.04 (Kearse et al., 2012) using
182 five iterations of the default mapper set to the highest sensitivity. The extracted consensus
183 sequence resulted in a 16,650 bp assembly of the *N. macropterus* mitogenome. The
184 mitogenome was then annotated using the MitoAnnotator web interface (Iwasaki et al.,
185 2013). Sequences of mitochondrial origin were then filtered out of the Illumina reads as
186 follows: first, bwa-kit v0.7.15 (Li & Durbin, 2009) was used to align the Illumina reads to the
187 indexed *N. macropterus* reference mitogenome with default parameters. Among other
188 aligners, the BWA-MEM algorithm (Li, 2013) was selected because it is the most accurate for
189 this type of short-read data (Keel & Snelling, 2018). In the resulting SAM alignment, 0.46% of
190 reads mapped to the mitogenome. Then, all the reads from the alignment that did not map
191 to the mitogenome were extracted to a new mitochondria-free alignment using SAMtools
192 v1.9 (Li et al., 2009) `view` with parameters `-b -f 4`, sorted by name, and finally converted
193 back to FASTQ paired-end reads with bedtools v2.27.1 (Quinlan & Hall, 2010).

194 2.6 Genome size estimation post-sequencing

195 Genome size and sequencing coverage based on the Illumina sequence reads was performed
196 with a *k*-mer frequency analysis. Total number of 17, 21, and 27-mers were counted with
197 jellyfish v2.2.10 (Marçais & Kingsford, 2011) command `count` and the resulting histograms
198 were computed with command `histo`. The histograms were analyzed with GenomeScope
199 (Vurture et al., 2017), which estimated a genome size of c. 516–520 Mb, with a high
200 heterozygosity level of 1.01–1.07 % and a duplication level of 0.98–1.10 % (

201 Figure 2, Supplementary Figure 1). This estimated haploid genome size was consistent, albeit
202 c. 150 Mb lower than the size estimated pre-sequencing. However, it is common for *k*-mer
203 estimated size and genome assembly size to be smaller than the size estimated with C-value
204 (Austin et al., 2017; Feron et al., 2020; Jansen et al., 2017). The heterozygous coverage of 40×
205 was considered sufficient for performing genome assembly.



206
207 Figure 2. Histogram of 21-mer frequency in Illumina reads. Estimation of genome size,
208 heterozygosity, and duplicated regions. The first and second peaks show the *k*-mer frequency

209 of heterozygous and homologous regions, respectively. See Supplementary Figure 1 for 17-
210 and 21-mer models.

211 2.7 Nanopore reads sequencing and filtering

212 A total of 99.18 Gb was obtained from the raw unfiltered reads, with an average read length
213 above 6 Kb and a maximum length above 1 Mb (Table 1). Quality control of the raw reads was
214 performed with NanoPack v1.0.0 (De Coster et al., 2018) using NanoStat on both FASTQ
215 reads and Albacore summary files. Nanopore reads were filtered and trimmed with
216 NanoFilt by applying a minimum length cut-off of 500 bases (Tan et al., 2018), a minimum
217 average read quality score of 7 (c. 80% base call accuracy), and removing the first 50
218 nucleotides following the author's recommendations (De Coster, 2017). Given that quality
219 values based on summary files were slightly lower overall than when based on reads (as
220 expected, c.f. github.com/wdecoster/nanofilt), the quality filtering was done based on the
221 summary file values to be more stringent. Filter-trimmed reads from both cells were merged
222 into a single FASTQ file.

223 2.8 Illumina + Nanopore hybrid assembly

224 *De novo* genome assembly of short and long reads was performed with the Maryland Super-
225 Read Celera Assembler pipeline, MaSuRCA (Zimin et al., 2013; Zimin, Puiu, et al., 2017). This
226 is one of the most common assemblers for performing short and long reads hybrid genome
227 assemblies of eukaryotes, with consistently good results across studies (Jiang et al., 2019; Tan
228 et al., 2018; Thai et al., 2019). In brief, MaSuRCA typically works as follows: Illumina paired-
229 end short reads are first assembled into non-ambiguous super-reads, which are then mapped
230 to Nanopore reads to further assemble them in long, high-quality pre-mega-reads. If there
231 are gaps between mega-reads in respect to their mapping to the Nanopore reads, these gaps
232 are filled with the Nanopore read sequence only if the Nanopore read stretch meets some
233 minimum criteria of coverage and quality to produce the mega-reads. If there are still gaps
234 that cannot be merged between mega-reads due to poor quality of the Nanopore sequence,

235 regions flanking these gaps are linked together as linking pair mates. The mega-reads and
236 linking pairs are then assembled with either CABOG or Flye (see below).

237 Before assembly, the filtered Illumina reads were not trimmed or edited as per MaSuRCA
238 author recommendation (<https://github.com/alekseyzimin/masurca>). The hybrid Illumina +
239 Nanopore assembly was run on MaSuRCA v3.2.9 with recommended parameters, automatic
240 *k*-mer size computation, and a jellyfish hash size of 20,000,000,000 (`PE = pe 350 50,`
241 `NANOPORE, EXTEND_JUMP_READS = 0, GRAPH_KMER_SIZE = auto,`
242 `USE_LINKING_MATES = 0, USE_GRID = 0, GRID_BATCH_SIZE =`
243 `300000000, LHE_COVERAGE=25, MEGA_READS_ONE_PASS=0,`
244 `LIMIT_JUMP_COVERAGE = 300, CA_PARAMETERS = cgwErrorRate = 0.15,`
245 `KMER_COUNT_THRESHOLD = 1, CLOSE_GAPS = 1, NUM_THREADS = 32,`
246 `JF_SIZE = 20000000000, SOAP_ASSEMBLY = 0`). MaSuRCA v3.2.9 uses a modified
247 version of the CABOG assembler (Miller et al., 2008) for the final assembly of corrected mega-
248 reads. However, later releases of MaSuRCA included the Flye assembler (Kolmogorov et al.,
249 2019) as a supposedly faster and more accurate alternative tool for the same step. To
250 compare both methods, a second assembly was run on MaSuRCA v3.4.1 with the same
251 parameters as above, but this time using `FLYE_ASSEMBLY = 1`. The Flye assembly was
252 subsequently polished with POLCA (Zimin & Salzberg, 2020) as implemented in MaSuRCA
253 v3.4.1 on default settings, using the clean Illumina reads to fix substitutions and indel errors.

254 2.9 HiFi sequencing and assembly

255 HiFi reads were converted from BAM to FASTA and FASTQ with SMRTLink v9.0 (PacBio, 2020)
256 `bam2fastx`. Assembly was performed with hifiasm v0.13 (Cheng et al., 2021) using default
257 parameters. The primary contigs were extracted from the GFA graph and converted to FASTA
258 with command `awk '/^S/{print ">"$2;print $3}'`. Another assembly was also
259 tentatively performed with HiCanu as implemented in Canu v2.1.1 (Nurk et al., 2020), with an
260 estimated genome size of 600 Mb. However, the read coverage estimated (6.68×) was lower
261 than the minimum coverage allowed by HiCanu (10×), so the assembly could not be
262 completed.

263 2.10 Quality assessment and comparison of assemblies

264 After each assembly, basic contiguity statistics were computed with `bbmap v38.31` (Bushnell,
265 2018) script `stats.sh`. Length, GC content, and GC skew of scaffolds in all assemblies were
266 also reported with `seqkit v0.10.1` (Shen et al., 2016) command `fx2tab`. To assess the
267 completeness of the assemblies, the Benchmarking Universal Single-Copy Orthologs (BUSCO)
268 tool v3.0.2 (Simão et al., 2015) was used with parameter `-sp zebrafish` on the
269 Actinopterygii odb9 orthologs set, which contains 4,584 single-copy orthologs that are
270 present in at least 90% of ray-finned fish species. Augustus v3.3.1 (Stanke et al., 2004), NCBI
271 blast+ v2.7.1 (Camacho et al., 2009), hmmer v3.2.1 (Eddy, 2011), and R v3.6.0 (R Core Team,
272 2020) were also required to run the BUSCO shell script.

273 The quality of the CABOG and Flye assemblies was further compared by mapping clean
274 Illumina reads back to the assemblies themselves with `bwa-kit v0.7.15` using `bwa mem -a`
275 `-M`. The resulting alignment files were also used to plot Feature Response Curves (FRC) (Vezi
276 et al., 2012b) with `FRCbam v5b3f53e-0` (Vezi et al., 2012a). This allowed comparison of
277 quality of the assemblies without relying on contiguity, by plotting the accumulation of error
278 “features” along the genome (e.g. areas with low or high coverage, number of unpaired reads,
279 misoriented reads). The presence of unmerged haplotigs in the CABOG and the Flye polished
280 assembly was investigated by using `minimap v2.16` (Li, 2018) with parameters `-ax map-`
281 `ont --secondary = no` to map the clean Nanopore reads back to the assembly and
282 then analyzing the resulting alignment with `Purge Haplotigs v1.1.1` (Roach et al., 2018)
283 command `hist`. The presence of trailing Ns in the Flye polished assembly was tested by using
284 `seqkit v0.10.1` command `-is replace -p "^n+|n+$" -r ""` and comparing the
285 input and the output.

286 A last quality check of the CABOG and Flye polished assemblies was done by plotting
287 assemblies against each other and against two chromosome-level fish assemblies using
288 `MashMap 2.0` (Jain et al., 2018) with a minimum mapping segment length of 500 bp and a
289 minimum identity of 85% (for comparison between tarakihi assemblies) and 90% (for

290 comparison between different species). To visualize the presence of potential misassemblies
291 on the longest scaffolds, the results from MashMap were used to plot the mappings of these
292 scaffolds between different assemblies with a custom R script (`plot_mashmap_scaffolds.R`).
293 The first fish chromosome-level assembly used for comparison was the mandarin fish
294 *Siniperca chuatsi* (SinChu7, GCA_011952085.1) because it was the phylogenetically closest
295 chromosome-level assembly (Centrarchiformes, Centrarchoidei) available on NCBI at the time
296 this analysis was performed. The second was the Australasian snapper *Chrysophrys auratus*
297 (SNA1, <https://www.genomics-aotearoa.org.nz/data>), in order to compare with a well-
298 curated specimen from a more evolutionarily distant species.

299 Final visualization of contiguity and completeness of the genome assemblies was generated
300 with `assembly-stats v17.02` (Challis, 2017) as implemented in the `gpiccoli` container (Piccoli,
301 2021).

302 2.11 Estimation of heterozygosity

303 The heterozygosity of TARdn1 was estimated a second time by calling SNPs from the Illumina
304 reads aligned to the final assembly. The reads were mapped to the polished assembly with
305 `bwa-kit v0.7.15` using the command `bwa mem -a -M`. Duplicates were marked with `picard`
306 `v2.18.20` (Broad Institute, 2019) `MarkDuplicates`. SNPs were called using `bcftools v1.9`
307 (Li, 2011) commands `mpileup (-C50 -q10 -incl-flags 2)` and `call (-m --`
308 `variants-only -- skip-variants indels)`. To filter for good quality SNPs,
309 variants depth distribution was plotted. The modal depth of coverage was 82, with an
310 increase in steepness starting at c. 20 and a decrease starting at c. 120 (Supplementary Figure
311 2). Consequently, the final SNP set was filtered with `vcftools v0.1.16` (Danecek et al., 2011)
312 for a minimum reference allele frequency of 0.25, a genotype depth of minimum 20 and
313 maximum 120, and a minimum site quality of 20.

314 2.12 Genome repetitive elements detection

315 Repetitive elements (RE) in the *N. macropterus* genome were identified both by *de novo*
316 modeling and based on repeats homology. RepeatModeler v2.0.1 (Flynn et al., 2020), as
317 implemented in Dfam TE Tools container v1.2 ([https://github.com/Dfam-](https://github.com/Dfam-consortium/TETools)
318 consortium/TETools), was used to identify repeat models *de novo* using parameter -
319 LTRStruct to include the detection of long terminal repeat retrotransposons. For the
320 homology-based library, RepeatMasker v4.1.1 (Smit et al., 2013) tool famdb.py was used
321 to obtain known Actinopterygii repeats from the combined total Dfam v3.3 (Storer et al.,
322 2021) and RepBase RepeatMasker Edition v20181026 (Bao et al., 2015) databases, using
323 parameters --ancestors -descendants --include-class-in-name --add-
324 reverse-complement. Both *de novo* and homology-based repeat libraries were then
325 concatenated in a custom repeat library for *N. macropterus*. The genome assembly sequences
326 were then mapped against the custom repeat library with RepeatMasker v4.1.1 (-gff -
327 xsmall) to classify repeat regions, create a repeat annotation file, and produce a “soft-
328 masked” (i.e. masked bases in lower case) genome assembly. An alternate “hard-masked”
329 assembly was also created by converting lower cases in the soft-masked assembly into Ns.

330 2.13 Iso-Seq analysis

331 Iso-Seq sub-reads were processed with the SMRTLink v9.0 Iso-Seq pipeline. Circular
332 consensus sequences were generated from the sub-reads with command ccs using a
333 minimum read quality (RQ) of 0.9. Clontech and NEB primers removal and de-multiplexing
334 were performed using lima with parameters --isoseq --dump-clips --peek-
335 guess. Poly-A tails were trimmed and concatemers were removed with isoseq3
336 refine. At that point, BAM files containing sequence reads from the four tissues were
337 merged in one. Clustering and polishing of full-length reads were performed with isoseq3
338 cluster and parameter --use-qvs to obtain a dataset of high-quality isoforms with a
339 predicted accuracy > 0.99. These high-quality polished isoforms were then aligned to the
340 unmasked *N. macropterus* genome with pbmm2 (--preset ISOSEQ --sort).

341 Subsequently, redundant isoforms were collapsed into non-redundant transcripts loci using
342 the command `collapse`. Non-redundant transcripts were screened for REs against the *N.*
343 *macropterus* custom repeat library with RepeatMasker v4.1.1. Transcripts with $\geq 70\%$ bases
344 masked were considered REs. Identified REs were discarded from further analyses using a
345 custom bash script for filtering (`Count_filter_N_isoseqrepeats.bash`) and categorized using a
346 custom R script (`R_characterize_transcripts.R`).

347 Alternative splicing (AS) events in the repeat-cleaned Iso-Seq reads were counted and
348 classified with SUPPA v2.3 (Trincado et al., 2018) with default parameters. These results were
349 compared with reported AS values for other animal species from studies that also used SUPPA
350 on Iso-Seq reads. Results reported were compiled for the zebrafish (*Danio rerio*) (Nudelman
351 et al., 2018), the goldfish (*Carassius auratus auratus*) (Gan et al., 2021), the Wuchang bream
352 (*Megalobrama amblycephala*) (Chen et al., 2021), the whiteleg shrimp (*Litopenaeus*
353 *vannamei*) (X. Zhang et al., 2019), and the cave nectar bat (*Eonycteris spelaea*) (Wen et al.,
354 2018).

355 2.14 Genome annotation

356 The unmasked *N. macropterus* genome was annotated using the MAKER v2.31.10 (Holt &
357 Yandell, 2011) pipeline. First, the simple repeats were filtered out of the repeats annotation
358 file with a custom bash script (`rm_simple_repeats.bash`) to retain only complex repeats. Only
359 complex repeats were kept because MAKER will hard-mask every region provided in the
360 repeats annotation file before running, discarding them from the gene detection process.
361 However, simple repeats should be available for gene annotation because low-complexity
362 regions are expected within many genes. Hard-masking only complex repeats regions as a
363 first step allows MAKER to subsequently identify and soft-mask the simple repeats regions
364 internally. Gene matches that start in a non-masked region but extend in a soft-masked region
365 can then be taken into account in the gene detection process. A first round of MAKER was run
366 on the unmasked genome using the high-quality, non-redundant, non-repetitive Iso-Seq
367 transcripts to infer gene predictions (`est2genome = 1`). For repeat masking during this

368 step, the complex repeats GFF file was provided for hard masking and only simple repeats
369 were annotated (`model_org = simple`). All GFF and FASTA outputs were then merged
370 with `ggf3_merge` and `fasta_merge`. Training files for the *ab initio* gene predictors
371 SNAP v2013.11.29 (Korf, 2004) and Augustus v3.3.1 (Stanke et al., 2004) were generated
372 based on round 1 results. For SNAP, only gene models with a maximum Annotation Edit
373 Distance (AED) of 0.25 and a minimum protein length of 50 were used. For Augustus, all the
374 regions that contain mRNA annotations, including the 1,000 surrounding bp, were extracted
375 to a FASTA file using a custom bash script (`augustus_rndx.bash`). BUSCO v3.0.2 was then run
376 in “genome” mode on the FASTA file using the *Actinopterygii odb9* orthologs set, the zebrafish
377 as initial HMM model, and parameter `--long` to self-train Augustus. MAKER was then run a
378 second time using SNAP and Augustus training files, as well as the Iso-Seq transcriptome and
379 repeats alignments as evidence (`est2genome = 0`). For this, all lines containing
380 “est2genome” and “repeat” in the merged GFF from round 1 were extracted and copied in
381 two files that were provided as evidence with the parameters `est_gff` and `rm_gff`,
382 respectively. Additionally, gene predictions were also inferred from protein homology during
383 this round (`protein2genome = 1`), by using protein sequences of zebrafish (*Danio rerio*),
384 three-spined stickleback (*Gasterosteus aculeatus*), spotted gar (*Lepisosteus oculatus*), Nile
385 tilapia (*Oreochromis niloticus*), medaka (*Oryzias latipes*), Japanese puffer (*Takifugu rubripes*),
386 green spotted puffer (*Tetraodon nigroviridis*), and southern platyfish (*Xiphophorus*
387 *maculatus*) that were downloaded from Ensembl release version 103 (Kersey et al., 2016).
388 After that, SNAP was trained again using the results from round 2, and a third run was
389 performed by using the *ab initio* training files, as well as the extracted repeats, Iso-Seq, and
390 protein homology GFF files as evidence. Genes were renamed with MAKER
391 `maker_map_ids` and `map_x_ids`.

392 All proteins predicted from the second round of MAKER were blasted against the NCBI non-
393 redundant protein sequences database (NR) with `blastp (-evalue 1e-6 -max_hsps 1`
394 `-max_target_seqs 1 -outfmt 6)` as implemented in blast+ v2.6.0. All putative gene
395 functions based on the best homology matches were annotated in the genome with a custom
396 bash script (`add_blast_annotation_custom.bash`). Protein-coding genes were also searched

397 for protein domains and signatures and annotated for InterPro (IPR), Pfam, and Gene
398 Ontology (GO) terms using InterProScan v5.50-84.0 (Jones et al., 2014) and MAKER
399 `ipr_update_gff`. Protein domains were exported as features in a GFF file using MAKER
400 `iprscan2gff3`.

401 Finally, low-quality genes were identified with AGAT v0.6.0 (Dainat, 2021). These genes were
402 filtered out if they were shorter than 50 amino acids and flagged if they had an incomplete
403 open reading frame (ORF). Gene models produced by the second MAKER round were kept as
404 the final reference dataset based on their higher number, AED distribution, and BUSCO
405 completeness (Supplementary Table 2). Genome annotation was also inspected visually with
406 JBrowse v1.1.10 (Skinner et al., 2009).

407 2.15 General bioinformatics tools

408 After each assembly, scaffolds were sorted by size using `seqkit v0.10.1` command `sort -l`
409 `-r -2` and renamed with command `replace -p .+ -r "{nr}"` (i.e. scaffold “1”
410 being the longest, etc.). All alignment files were systematically sorted by leftmost coordinates,
411 converted to BAM, and indexed with SAMtools v1.9. Alignment summary reports were
412 produced with BAMtools v2.5.1 (Barnett et al., 2011). FASTQ files were converted in FASTA
413 when needed with `seqtk v1.3` (<https://github.com/lh3/seqtk>), and similarly, GFFs were
414 converted to GTF with AGAT v0.6.0. Analyses were performed on Rāpoi, the Victoria
415 University of Wellington high-performance computer cluster. Analyses requiring R scripts
416 were performed in R v4.02 (R Core Team, 2020) on RStudio (RStudio Team, 2020). All bash
417 and R scripts used for this chapter are available on GitHub on the following repository:
418 https://github.com/yvanpapa/tarakihi_genome_assembly.

419 3. Results

420 3.1 Genome sequencing

421 Illumina sequencing reads filtering (i.e. quality, contamination, and mitochondria) resulted in
422 a final dataset of 54.91 Gb short reads (Table 1) with a c. 92× depth of coverage. The GC
423 content was 43% and the overall sequence read quality was high. Both forward and reverse
424 reads passed all the FastQC criteria, i.e. they were never flagged for poor quality
425 (Supplementary Figure 3). Although there was a small bias in per base sequence contents of
426 the first c. 10 bases, this was expected due to the non-random nature of the hexamer priming
427 step during sequencing (Hansen et al., 2010). This slight deviation from uniformity in
428 sequence content was not considered an issue because there is no quantitative step involved
429 in the analyses based on the short reads. Nanopore sequencing, filtering, and trimming
430 resulted in 9.18 million reads (73.39 Gb), or 122× coverage, with an average read length of 8
431 Kb (Table 1), a mean read quality of 7.9, and an N50 length of 9.5 Kb. A total of 285,997 CCS
432 Hi-Fi reads (4.01 Gb) and 91,602 repeat-free, non-redundant, high-quality Iso-Seq transcripts
433 (312.31 Mb) were also obtained.

434 Table 1. Summary of number, base quantity, and length of reads obtained at several steps of
435 the quality filtering pipelines.

Reads	Number of reads	Total number of bases	Minimum read length	Average read length	Maximum read length
Raw Illumina PE reads	425,740,632	63,861,094,800	150	150	150
Quality-filtered Illumina PE reads	405,228,300	60,784,245,000	150	150	150
Uncontaminated Illumina PE reads	367,760,592	55,164,088,800	150	150	150
Final Illumina PE reads	366,065,036	54,909,755,400	150	150	150
Raw Nanopore reads cell 1	8,270,853	52,169,467,195	5	6,307.6	1,029,695
Raw Nanopore reads cell 2	7,229,556	47,015,342,634	5	6,503.2	1,035,919
Final Nanopore reads	9,178,726	73,394,980,774	450	7,996.2	182,445
HiFi reads	285,997	4,009,988,664	49	14,021.1	27,427
Iso-Seq sub-reads (4 tissues)	171,924,197	302,196,904,697	51	2,601.15	278,803
Final Iso-Seq transcripts	91,602	312,308,038	80	3,409.4	10,426

436 Notes: Reads in bold were the ones used in the final retained (Flye polished) assembly. Final Illumina
437 PE reads have been filtered for quality, DNA contamination, and mitochondrial DNA. Final Nanopore
438 reads have been filtered for quality. Final Iso-Seq CCS transcripts were filtered for quality and repeat
439 transcripts and were non-redundant.

440 3.2 Assemblies comparison and quality assessment

441 The Flye assembly reduced the number of scaffolds by more than half compared to the
442 CABOG assembly (Table 2). The scaffold N50 length of the Flye assembly was almost twice as
443 long and the number of complete BUSCOs was higher. The Flye assembly size was also more
444 consistent with the haploid genome size pre-estimated by *k*-mer counting (c. 520 Mb) than
445 the CABOG assembly. Interestingly, the Flye assembly also corrected a misassembly of the
446 first scaffold of the CABOG assembly (see below). Polishing the Flye assembly resulted in the
447 correction of 43,080 substitutions errors and 42,783 deletion errors. The polished assembly
448 had the same number of scaffold and contigs, but a few hundred fewer bases, and one missing
449 BUSCO was recovered into an additional single-copy BUSCO. The hifiasm assembly performed
450 on the HiFi reads did not produce satisfactory results compared to the Illumina + Nanopore
451 hybrid assemblies, with six to ten times more scaffolds, an N50 length 50 times smaller, and

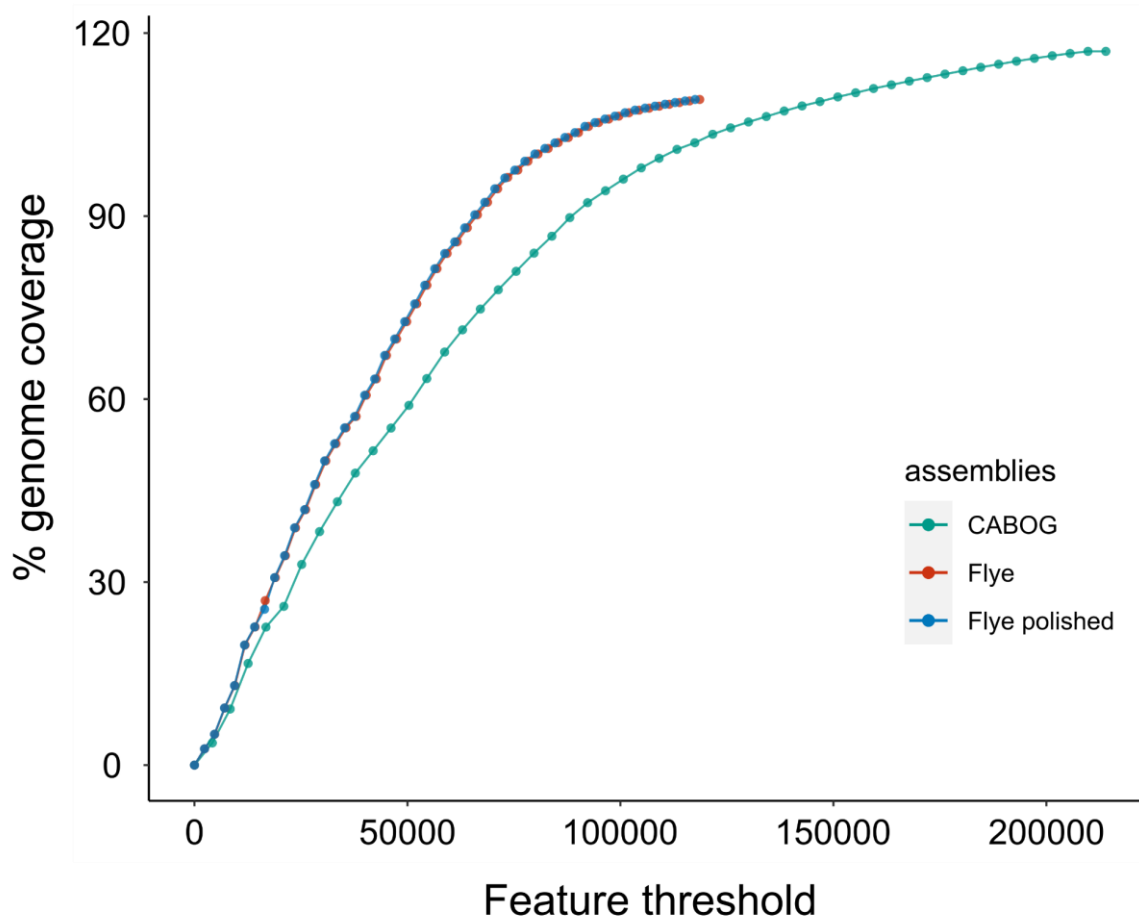
452 a BUSCO completeness lower than 90%. This was most probably due to the low coverage of
453 HiFi reads (c. 6.5x) used for this sequencing trial.

454 Table 2. General statistics of the four assemblies produced.

Reads type	PacBio HiFi reads	Illumina + Nanopore reads		
	hifiasm	CABOG	Flye	Flye polished
Genome Assembly				
Scaffold assembly size	778,095,731 bp	608,975,097 bp	567,903,348 bp	567,902,715 bp
Total number of scaffolds	13,511	2,696	1,214	1,214
Longest scaffold	469,394 bp	18,930,378 bp	13,913,512 bp	13,913,694 bp
Scaffold N50 / L50	67.836 Kb / 3,650	1.87 Mb / 69	3.37 Mb / 45	3.37 Mb / 45
Scaffold N90 / L90	30.868 Kb / 10,456	140.52 Kb / 535	437.51 Kb / 219	437.54 Kb / 219
Proportion of gap sequences	0.001%	0.002%	0.001%	0.001%
Contigs size	778.096 Mb	609.964 Mb	567.900 Mb	567.900 Mb
Total number of contigs	13,511	2,809	1,245	1,245
Contig N50 / L50	67.836 Kb / 3,650	1.79 Mb / 74	2.94 Mb / 52	2.94 Mb / 52
Contig N90 / L90	30.868 Kb / 10,456	137.36 Kb / 556	429.99 Kb / 242	429.98 Kb / 242
A / T / G / C / bases (%)	28.17 / 28.14 / 21.84 / 21.85	28.06 / 28.13 / 21.91 / 21.90	28.10 / 28.15 / 21.87 / 21.88	28.10 / 28.15 / 21.87 / 21.88
GC standard deviation	2.13%	5.87%	3.87%	3.87%
Genome Completeness (4,584 Actinopterygii BUSCOs)				
Complete BUSCOs	88.8%	97.6%	97.7%	97.8%
Complete single-copy BUSCOs	57.3%	92.9%	95.1%	95.2%
Complete duplicated BUSCOs	31.5%	4.7%	2.6%	2.6%
Fragmented BUSCOs	3.5%	0.8%	0.8%	0.8%
Missing BUSCOs	7.7%	1.6%	1.5%	1.4%

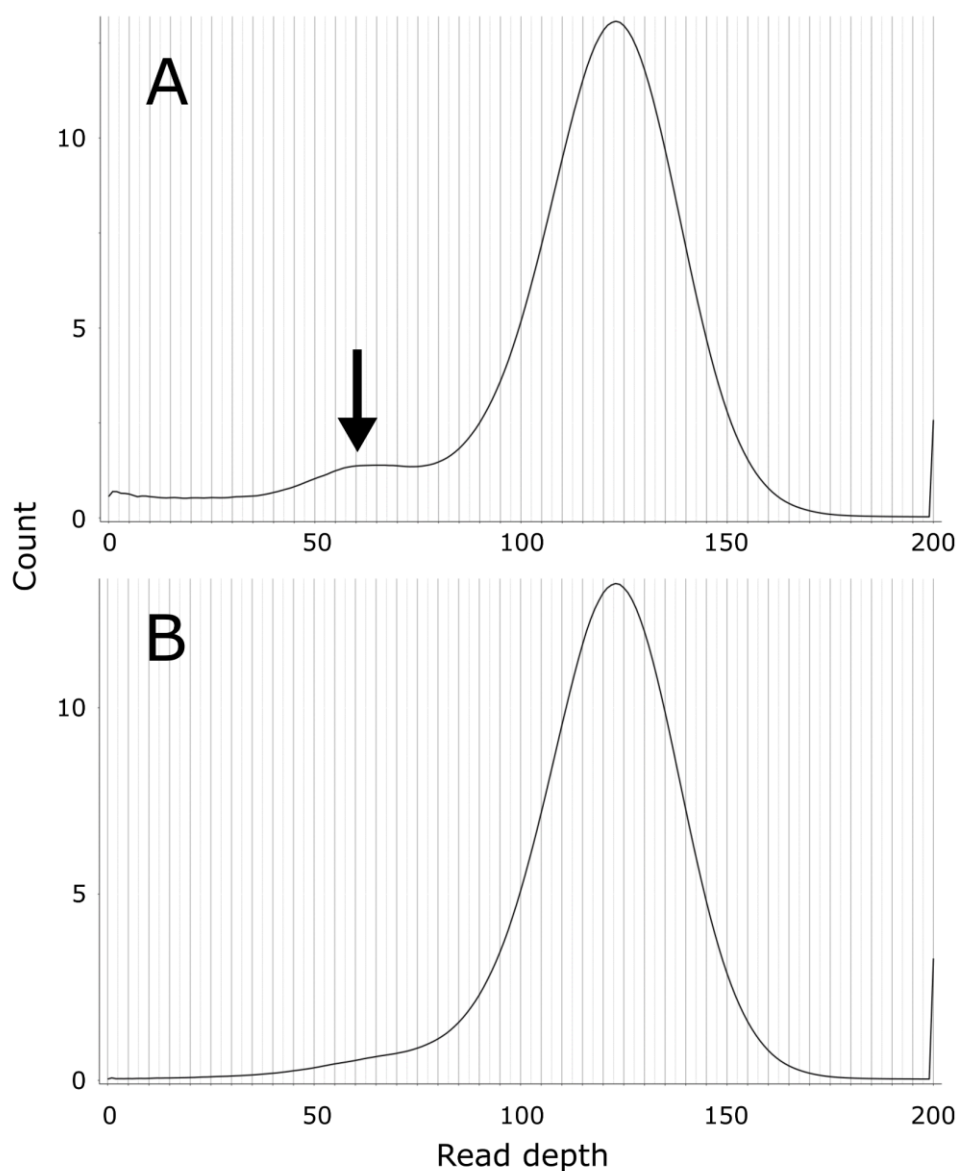
455 Note: The Flye polished assembly (in bold) yielded the best results and was retained for all subsequent analyses.

456 Approximately 99.7% of Illumina reads could be mapped back to the CABOG assembly, and
457 99.8% to both Flye assemblies, making the Flye assemblies slightly more accurate according
458 to that metric. The Flye polished assembly had a slightly higher proportion of “proper-pairs”
459 reads mapped (86.23%) than the un-polished assembly (85.7%). FRC curves showed that both
460 Flye assemblies were more accurate than the CABOG assembly (Figure 3). Moreover, while
461 both the unpolished and polished Flye assemblies have a very similar curve, for the same
462 genome coverage, the polished Flye assembly always had a slightly lower amount of
463 cumulative errors compared to the un-polished assembly (Supplementary Figure 4.).



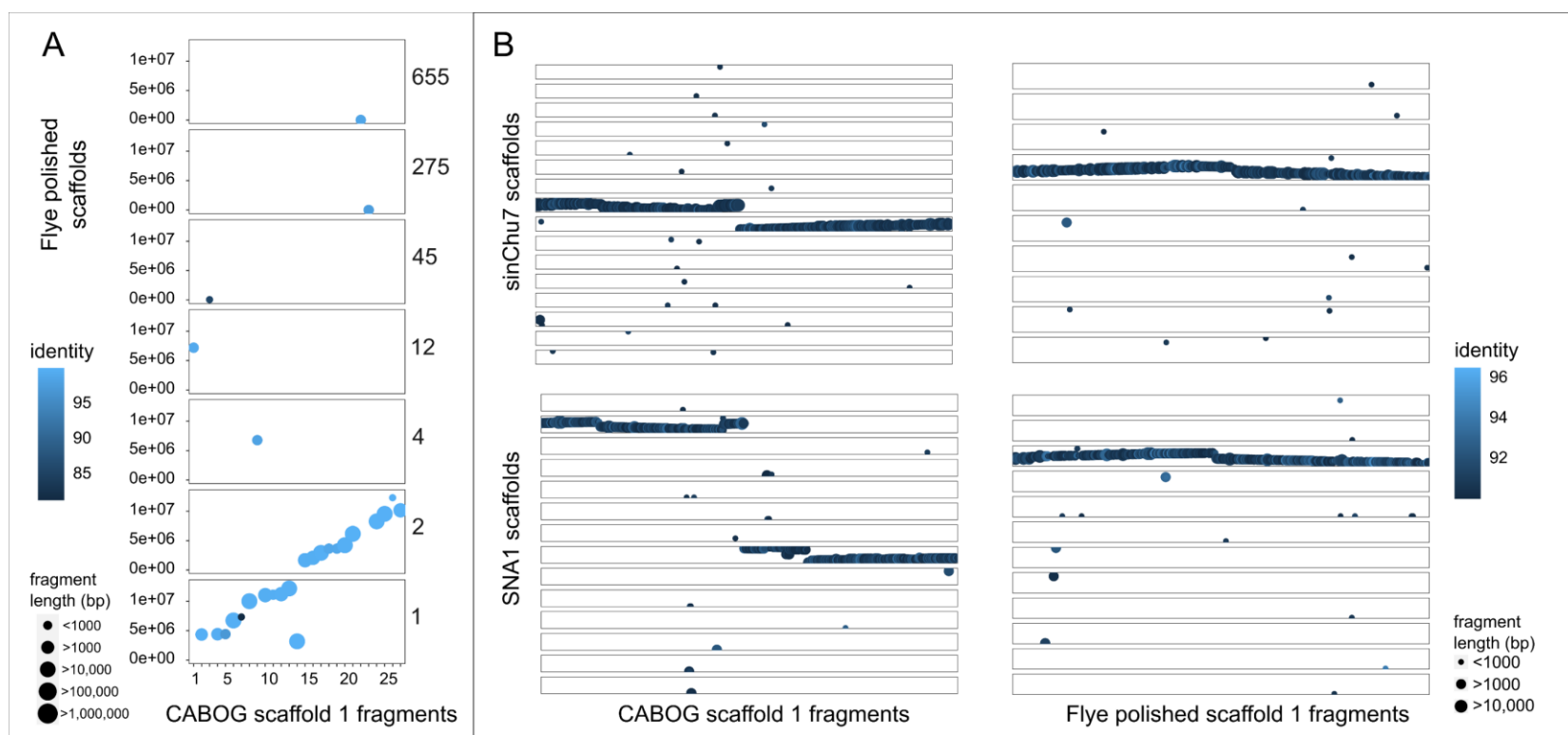
464
465 Figure 3. FRC curves for the CABOG, Flye, and Flye polished assembly. The Y-axis represents
466 the cumulative size of the assembly and the X-axis is the cumulative number of potential
467 errors (i.e. “features”). Assemblies for which the curves are steeper are considered more
468 accurate.

469 While there was evidence of the presence of unmerged haplotigs in the CABOG assembly
470 (Figure 4A), none were detected in the Flye polished assembly (Figure 4B), thus a filtering step
471 was not required. Trailing Ns were not present in the Flye polished assembly either.



472
473 Figure 4. Read depth histograms of the genome assemblies contigs, obtained by mapping the
474 clean Nanopore reads back to the assembly. A unimodal distribution with a peak equal to the
475 sequencing reads depth is expected for a haplotig-free assembly. Another peak at half of the
476 sequencing reads depth (arrow) is indicative of the presence of unmerged haplotigs. A:
477 CABOG assembly B: Flye polished assembly.

478 Interestingly, the longest scaffold of the CABOG assembly, scaffold 1, was 5 Mb longer than
479 the longest scaffold of the Flye assembly (Table 2). Between-scaffolds alignment scores
480 obtained from MashMap (Supplementary Figure 5) were used to visualize a potential
481 misassembly at that scaffold. The longest scaffold of the CABOG assembly corresponded
482 indeed to the two longest scaffolds of the polished Flye assembly, scaffolds 1 and 2 (Figure
483 5A). The CABOG scaffold 1 is highly likely to have been misassembled since it also corresponds
484 to two long regions in two different linkage groups (i.e. chromosomes) in both chromosome-
485 level assemblies of *S. chuatsi* and *C. auratus*. This is not the case for scaffold 1 in the polished
486 Flye assembly (Figure 5B). This supported the interpretation that the “correct” longest
487 scaffold is the one from the polished Flye assembly.

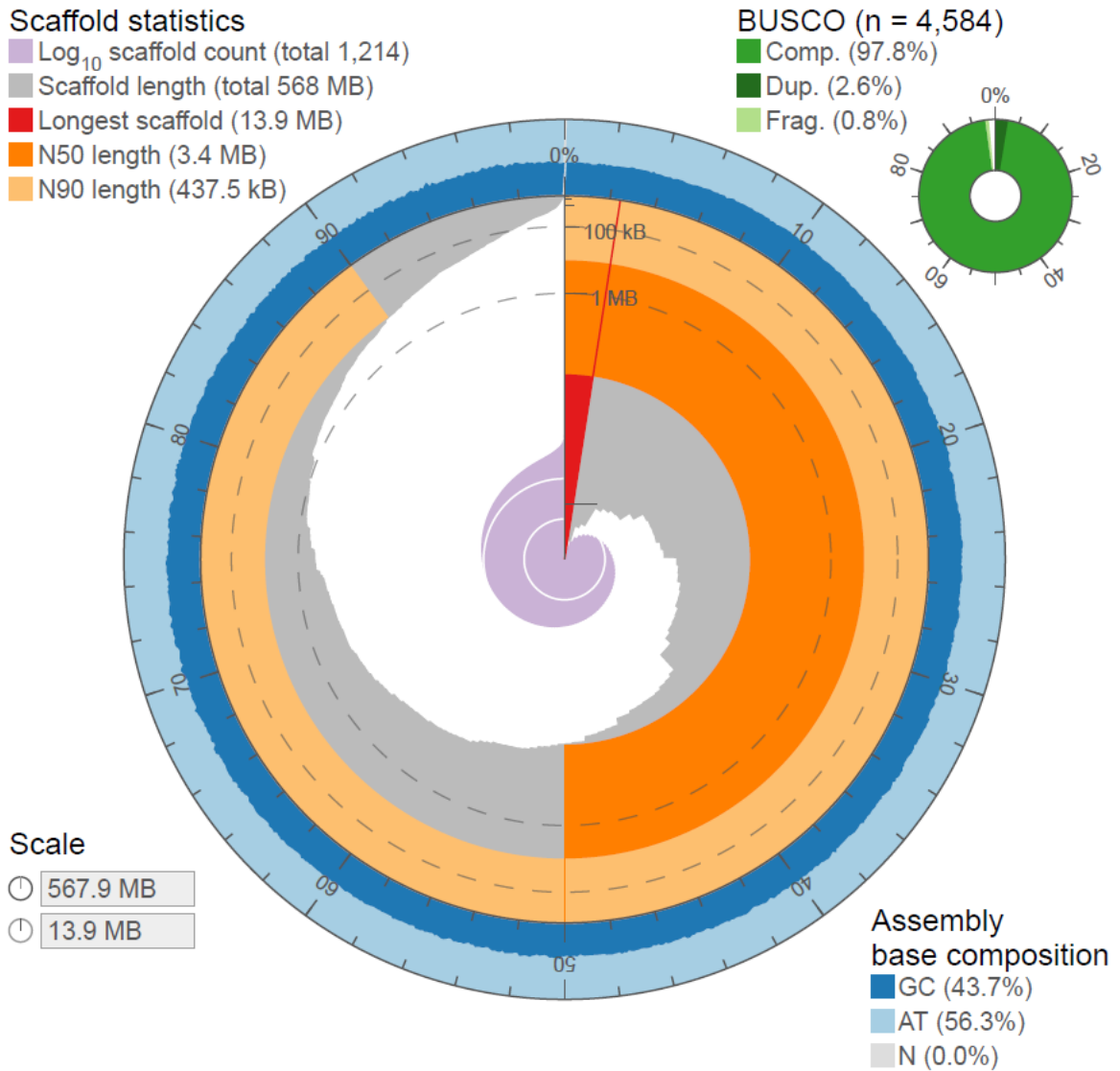


488
489

490 Figure 5. Scaffolds plotted against total assemblies based on identity results from MashMap with minimum mapping region (i.e. “fragments”)
491 length of 500bp. Each horizontal box is a scaffold of the reference on which the query scaffolds are mapped according to a given identity
492 threshold. Mapped regions are ordered by base coordinate along the query scaffold on the x-axis, and the reference scaffolds on the y-axes. (A)
493 CABOG assembly scaffold 1 mapped to the total polished Flye assembly, with corresponding Flye scaffold numbers reported on the right. (B)
494 CABOG and Flye assemblies scaffold 1 mapped to the *S. chuatsi* and *C. auratus* chromosome-level assemblies.

495 3.3 Final assembly statistics

496 The Flye polished assembly provided the best results and thus was used in all subsequent
497 analyses. This final genome assembly consisted of 567,902,715 bases in 1,214 scaffolds, with
498 a scaffold N50 length of 3.37 Mb and a proportion of gaps of 0.001% (Table 2, Figure 6). Base
499 composition was A: 28.10%, T: 28.15%, G: 21.87%, C: 21.88%, and overall standard deviation
500 of GC content was 3.87%. The BUSCO completeness was very good overall, with more than
501 95% of the single-copy Actinopterygii orthologs retrieved in the final assembly (Table 2, Figure
502 6). The contiguity and completeness were high when compared to other Illumina + Nanopore
503 hybrid assemblies (Table 3). The final assembly was named fNemMar1, in accordance with
504 the Earth Biogenome Project sample naming scheme ([https://gitlab.com/wtsi-grit/darwin-
505 tree-of-life-sample-naming](https://gitlab.com/wtsi-grit/darwin-tree-of-life-sample-naming)).



506

507 Figure 6. Visualization of contiguity and completeness of the final tarakihi assembly. The
508 contiguity is visualized in a circle representing the full assembly length of c. 568 Mb. The
509 longest scaffold was 13.9 Mb. There were very few scaffolds (c. 2%) shorter than 100 Kb in
510 length and the GC content was uniform throughout. See Supplementary Figure 6 for a
511 comparison with the three other assemblies that were not retained.

512 Table 3. Comparison of the contiguity and completeness of genomes that were assembled
513 using a hybrid approach including only short Illumina reads and long Nanopore reads.

Species	Genome (total scaffolds) length	Number of scaffolds	Scaffold N50 length	Complete BUSCOs	Protein-coding gene models	Functionally annotated genes
Tarakihi	568 Mb	1,214	3.4 Mb	97.80%	20,327	19,823
Murray cod	633 Mb	18,198	0.1 Mb	94.20%	26,539	25,607
Clownfish	881 Mb	6,404	0.4 Mb	96.30%	27,420	26,211
<i>Danionella translucida</i>	735 Mb	27,639	0.3 Mb	91.50%	24,097	21,491
Snout otter clam	544 Mb	622	2.1 Mb	95.80%	26,380	23,701
Indian blue peacock	915 Mb	15,025	0.2 Mb	not reported	23,153	21,854

514 Note: All fish genome assemblies that corresponded to the criteria are reported (Murray cod
515 (*Maccullochella peelii*): Austin et al. (2017), clownfish (*Amphiprion ocellaris*): Tan et al. (2018),
516 *Danionella translucida*: Kadobianskyi et al. (2019)) and two selected additional species have been
517 included for comparison with other groups of organisms (Mollusc, snout otter clam (*Lutraria*
518 *rhynchaena*): Thai et al. (2019); bird, Indian blue peacock (*Pavo cristatus*): Dhar et al. (2019)).

519 3.4 Estimation of heterozygosity

520 Variant calling of Illumina reads against the polished assembly resulted in a total of 3,654,819
521 SNPs. By dividing this number by the size of the genome, this corresponded roughly to a
522 heterozygosity level of 0.64%. This is lower than the level estimated by *k*-mer frequency (c.
523 1.00%). However, it is common for heterozygosity estimated by *k*-mer frequency to be lower
524 compared to called SNPs, because the SNP calling approach is more conservative (Thai et al.,
525 2019). Nevertheless, the heterozygosity estimated for TARdn1 is one of the highest reported
526 for a fish species. To our knowledge, this is the highest heterozygosity estimated for a fish
527 through *k*-mer analysis, with other reported values ranging from 0.1% (Tibetan loach
528 *Triplophysa tibetana* and Murray cod *Maccullochella peelii*) to 0.9% (Java medaka *Oryzias*
529 *javanicus*) (Austin et al., 2017; Ge et al., 2019; Gong et al., 2018; Lu et al., 2020; Nguinkal et
530 al., 2019; Takehana et al., 2020; Vij et al., 2016; Yang et al., 2019; H. H. Zhang et al., 2020;
531 Zheng et al., 2021). Even the heterozygosity estimated through SNPs (0.64%) is high compared
532 to estimations from other fish using the same method (e.g. large yellow croaker: 0.36% (Wu
533 et al., 2014), grass carp: 0.25% (Y. Wang et al., 2015)). This result is even more striking in that
534 the variant analysis was very stringent in our case by retaining only high-quality bi-allelic SNPs.
535 This reinforces the recent findings that *N. macropterus* is a species with a historically large
536 population that displays a particularly high genetic diversity (Papa, Halliwell, et al., 2021).

537 3.5 Repetitive elements and genes annotation

538 REs represented 30.45% of the genome, or a total of 172,911,032 bp. Although the proportion
539 of REs in fish genomes can vary greatly at scales from 10% to 60% (Yuan et al., 2018), the
540 proportion of repeat elements in *N. macropterus* is on par with the proportion observed in
541 other Centrarchiformes (Largemouth bass (*Micropterus salmoides*): 33.79%, Big-eyed
542 mandarin fish (*Siniperca kneri*): 26.55%) (Lu et al., 2020; Sun et al., 2021) and for Perciformes
543 in general (Yuan et al., 2018). Of the REs known in the databases, interspersed repeats
544 accounted for 27.62% of the genome, including 10.87% of DNA transposons and 6.17% of
545 retro-elements (LINEs, LTR, SINEs, and PLE in that order). The rest of the repeat elements
546 consisted of simple sequence repeats (Supplementary Table 1).

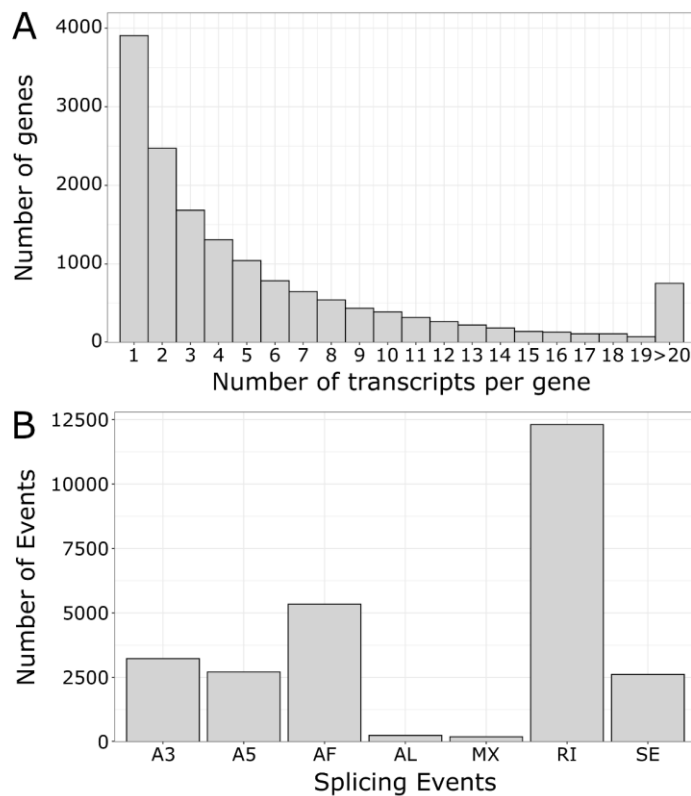
547 After filtering for length, the final predicted gene set included 20,169 protein-coding genes
548 with a mean length of 13,832 bp, among which 95.5% had an AED < 0.5. The mean exon length
549 was 229 bp, and the mean intron length in CDS was 1,184 bp. More than 98% of the genes
550 were functionally annotated by at least one of the two methods used (blastp 98.2%,
551 InterProScan 82.8%).

552 3.6 Iso-Seq analysis

553 Of the 93,949 full-length polished, non-redundant Iso-Seq transcripts, 2,347 were classified
554 as REs and were filtered out from downstream analyses. For each of these RE transcripts, the
555 main RE elements included DNA elements (801), LINEs (639), LTRs (464), SINEs (94), rRNAs
556 (47), low complexity / simple repeats (33), rolling circles (26), satellites (16), and retroposons
557 (2), as well as one LINE/LTR hybrid, and 224 unknown RE.

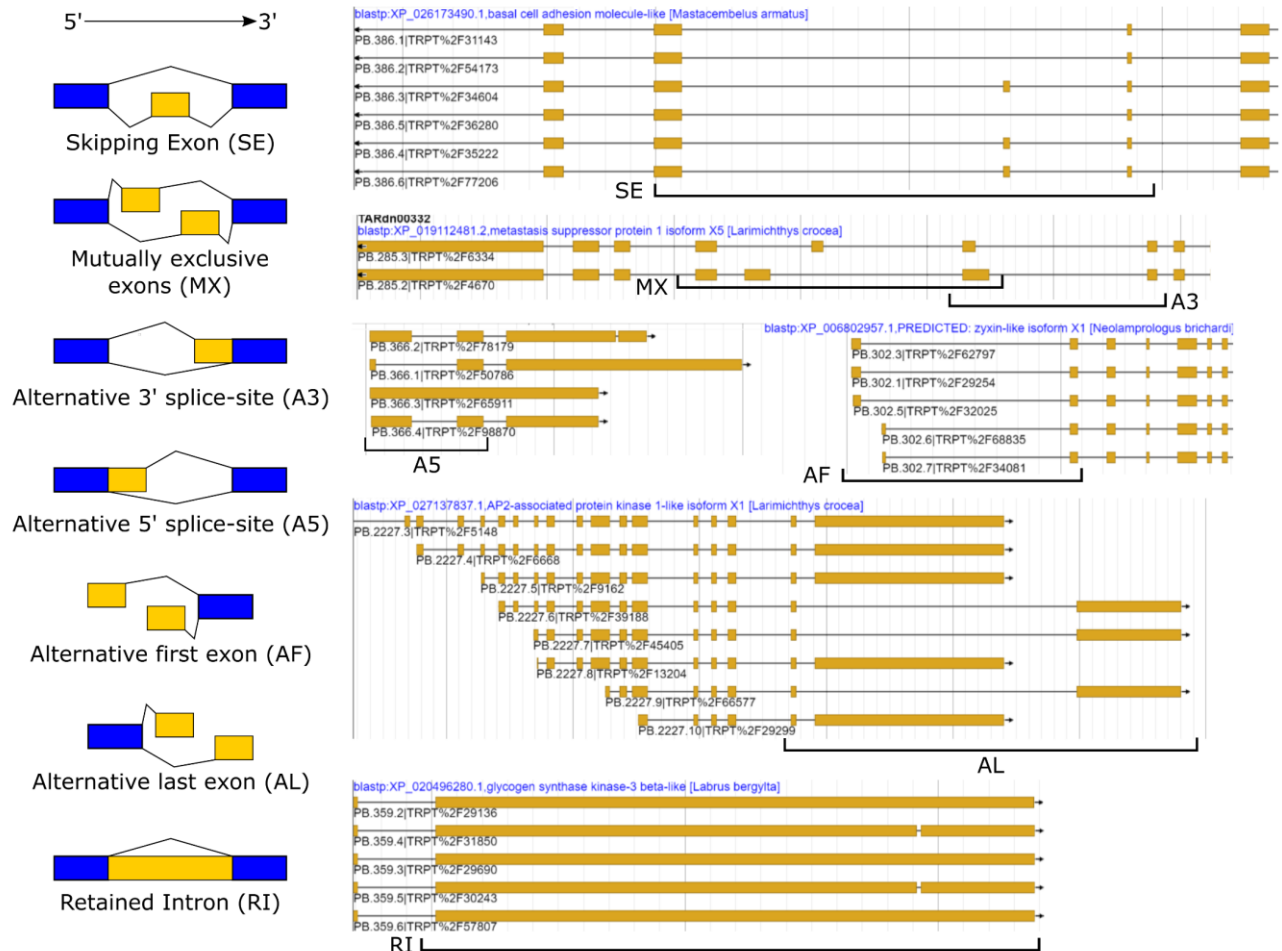
558 The final non-RE Iso-Seq dataset included 91,313 unique transcripts from 15,515 genes. The
559 mean transcript per gene ratio was 5.89, with a median of 3 and a maximum of 211 (Figure
560 7A). This is higher than the values recently reported for humans (3.62) and two species of bats
561 (1.92 and 1.49), but lower than pharaoh ants (9) (Q. Gao et al., 2020; Wen et al., 2018). Less
562 than 5% of genes had more than 20 different transcripts. The predicted proteins of both genes

563 that produced the most transcripts (respectively 211 and 164 transcripts) were collagen alpha
564 chains isoforms (XP_006787735.1: collagen alpha-2(I) chain-like isoform X2,
565 XP_020490299.1: collagen alpha-1(V) chain-like isoform X1), implicated in the structural
566 integrity of the cellular matrix (GO:0005201).



567
568 Figure 7. Alternative transcripts metrics in the tarakihi transcriptome (A) Number of unique
569 alternative transcripts per gene. (B) Classification and frequency of alternative splicing events.
570 A5/A3: Alternative 5'/3' Splice Sites. AF/AL: Alternative First/Last Exons. MX: Mutually
571 Exclusive Exons. RI: Retained Intron. SE: Skipping Exon.

572 A total of 26,644 AS events were detected in the tarakihi transcriptome (Figure 7B). The most
573 frequent AS event was the retention of intron (46%), while “alternative last exons” and
574 “mutually exclusive exons” were the rarest (less than 1% each). Some examples of these AS
575 events were visualized in the tarakihi genome (Figure 8).

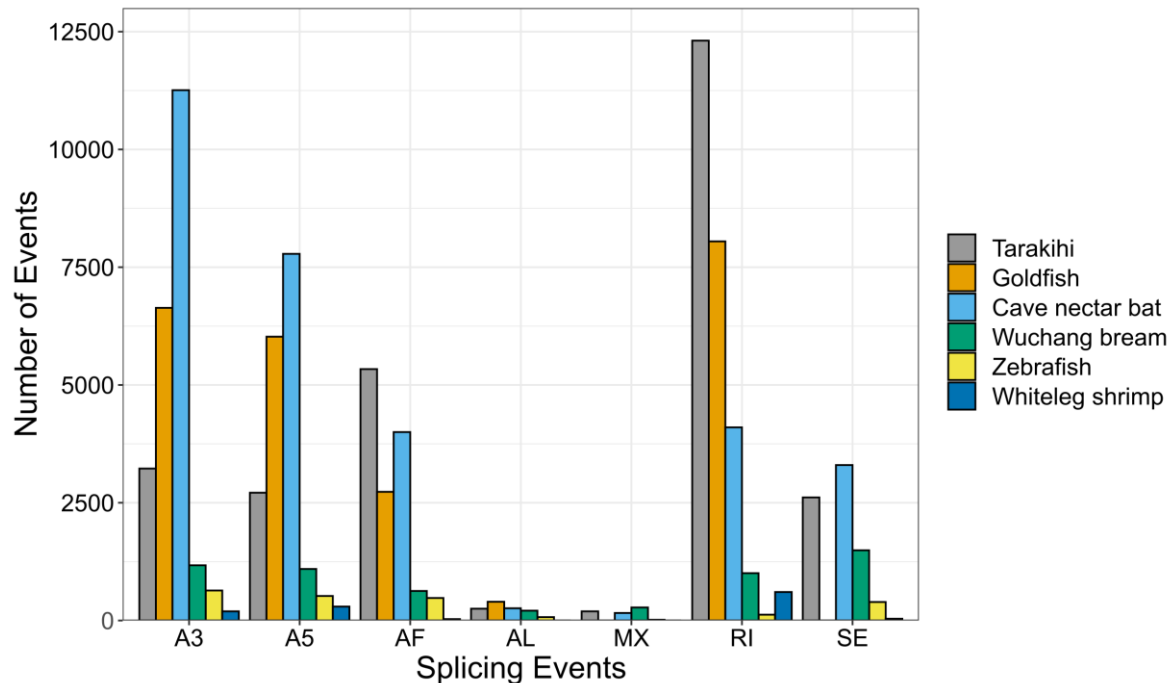


576

577 Figure 8. The seven types of alternative splicing events classified in the tarakihi transcriptome,
578 with examples of each event class as visually shown in the annotation of the genome.

579 Comparison of the frequency of AS events in the tarakihi with other species showed that the
580 trends are globally similar across organisms (Figure 9). Most organisms show relatively high
581 occurrences of RI, A3, A5, AF, and to a lesser degree SE, compared to AL and MX. The figure
582 also shows that tarakihi, goldfish, and cave nectar bat may have a better representation of
583 the AS events proportions due to a much deeper coverage compared to the Wuchang bream,
584 zebrafish, and whiteleg shrimp (although values for MX and SE were not reported for the
585 goldfish study). While it is the most common AS event in both tarakihi and goldfish, the
586 proportion of RI events is much higher in tarakihi compared to the proportion of other events.
587 While intron retention was thought until recently to be the least prevalent AS form in animals,
588 it is now clear that this is not the case (as shown in the studies in Figure 9 but also e.g. Q. Gao

589 et al. (2020); X. Wang et al. (2019)). RI events are widely used across organisms to tune down
590 the levels of transcription of some genes in cells and tissues depending on their function
591 (Braunschweig et al., 2014).



592
593 Figure 9. Comparison of alternative splicing event counts between tarakihi and five other
594 animal species from other Iso-Seq AS studies. MX and SE events were not reported in the
595 goldfish study.

596 3.7 Genome size

597 The size of the tarakihi genome was consistent with values for fish genomes that have been
598 reported so far. A recent review of publicly available fish genome assemblies (comprising 244
599 species) showed that the average genome length of fish is 872.64 Mb but varies between c.
600 300 Mb to c. 4.5 Gb (Fan et al., 2020). The genome size of *N. macropterus* (568 Mb) is several
601 hundred Mb shorter than the two other published Centrarchiforme genomes, the largemouth
602 bass *Micropterus salmoides* (964 Mb) and the big-eye mandarin fish *Siniperca kneri* (732.1
603 Mb) (Lu et al., 2020; Sun et al., 2021). However, *N. macropterus* is still evolutionarily far apart
604 from these two species. The largemouth bass and the big-eye mandarin fish both belong to

605 the Centrarchoidei sub-order, which is thought to have split from Cirrhitioidei at least 70
606 million years ago (Sanciango et al., 2016).

607 **4. Conclusion**

608 The advances in DNA sequencing technologies have made it clear how valuable reference
609 genome assemblies are for the study of biology and conservation, resulting in a global effort
610 to assemble the genomes of as many organisms as possible (Fan et al., 2020; Koepfli et al.,
611 2015; Worley et al., 2017). Here we present the first genome assembly of the tarakihi, a
612 valuable commercial fisheries species, and the first representative out of the c. 60 species of
613 the Cirrhitioidei suborder to have a whole genome sequenced. While performing a hybrid
614 assembly of Illumina and Nanopore reads with the latest tools led to a highly contiguous
615 assembly with high gene completeness, this could be still improved in the future by adding
616 Hi-C data to scaffold it to a chromosome-level assembly (Whibley et al., 2021). Moreover,
617 while PacBio HiFi data was a very new and still relatively expensive technology at the time of
618 data collection, it will probably replace the short and long reads hybrid assembly method as
619 the optimal genome assembly strategy by offering the best of both worlds (long reads and
620 high quality) and allowing phasing of genomes. However, the present genome and its
621 accompanying highly accurate transcriptome will still be a valuable resource for future
622 studies, including, but not restricted to comparative genomics, population structure analyses,
623 and the study of adaptive selection.

624 **5. Acknowledgments**

625 The authors are thankful to Igor Ruza, David Ashton, and Matthew Wylie (Plant and Food
626 Research, Nelson) for assisting in the sampling of the captive-bred specimen and to Nick
627 Johnston for capturing and providing the wild specimen. They are also grateful for advice and
628 assistance from the Removing Fisheries Juvenile Habitat Bottleneck Technical Advisory group,
629 and in particular, they wish to acknowledge the support and consultation from Laws Lawson
630 (Te Ohu Kaimoana), Jeremy Helson (Fisheries Inshore New Zealand), and Carol Scott

631 (Southern Inshore Fisheries Management Company Limited). They thank Tom Oosting and
632 Holly Jackson (Victoria University of Wellington) for proofreading the manuscript.

633 **6. CRediT authorship contribution statement**

634 **Yvan Papa:** Conceptualisation, Methodology, Software, Validation, Formal analysis,
635 Investigation, Resources, Data Curation, Writing - Original Draft, Writing - Review & Editing,
636 Visualisation. **Maren Wellenreuther:** Resources, Writing - Review & Editing, Supervision,
637 Funding acquisition. **Mark A. Morrison:** Writing - Review & Editing, Supervision, Funding
638 acquisition. **Peter A. Ritchie:** Conceptualisation, Resources, Writing - Review & Editing,
639 Supervision, Project administration, Funding acquisition.

640 **7. Disclosure statement**

641 No potential conflict of interest was reported by the authors.

642 **8. Funding**

643 This work was supported by the New Zealand Ministry of Business, Innovation and
644 Employment Endeavour Fund Research Programme [grant number CO1X1618] and a Victoria
645 University of Wellington Doctoral Scholarship.

646 **9. Data availability statement**

647 All genomic sequences and associated metadata are deposited on the Genomics Aotearoa
648 repository (<https://repo.data.nesi.org.nz/>) under project name "tarakihi genomics". All
649 scripts used in the analyses are openly available on GitHub at
650 https://github.com/yvanpapa/tarakihi_genome_assembly.

651 **10. References**

- 652 Aljanabi, S. M., & Martinez, I. (1997). Universal and rapid salt-extraction of high quality
653 genomic DNA for PCR- based techniques. *Nucleic Acids Research*, 25(22), 4692–4693.
654 <https://doi.org/10.1093/nar/25.22.4692>
- 655 An, D., Cao, H. X., Li, C., Humbeck, K., & Wang, W. (2018). Isoform sequencing and State-Of-
656 Art applications for unravelling complexity of plant transcriptomes. *Genes*, 9(1).
657 <https://doi.org/10.3390/genes9010043>
- 658 Andrews, S. (2018). *FastQC: A quality control tool for high through-put sequence data*.
659 <http://www.bioinformatics.babraham.ac.uk/projects/fastqc>
- 660 Austin, C. M., Tan, M. H., Harrisson, K. A., Lee, Y. P., Croft, L. J., Sunnucks, P., Pavlova, A., &
661 Gan, H. M. (2017). De novo genome assembly and annotation of Australia’s largest
662 freshwater fish, the Murray cod (*Maccullochella peelii*), from Illumina and Nanopore
663 sequencing read. *GigaScience*, 6(8), 1–6. <https://doi.org/10.1093/gigascience/gix063>
- 664 Babcock, R. C., Bustamante, R. H., Fulton, E. A., Fulton, D. J., Haywood, M. D. E., Hobday, A. J.,
665 Kenyon, R., Matear, R. J., Plagányi, E. E., Richardson, A. J., & Vanderklift, M. A. (2019).
666 Severe continental-scale impacts of climate change are happening now: extreme climate
667 events impact marine habitat forming communities along 45% of Australia’s coast.
668 *Frontiers in Marine Science*, 6, 1–14. <https://doi.org/10.3389/fmars.2019.00411>
- 669 Bao, W., Kojima, K. K., & Kohany, O. (2015). Repbase Update, a database of repetitive
670 elements in eukaryotic genomes. *Mobile DNA*, 6(1), 11. [https://doi.org/10.1186/s13100-](https://doi.org/10.1186/s13100-015-0041-9)
671 [015-0041-9](https://doi.org/10.1186/s13100-015-0041-9)
- 672 Barnett, D. W., Garrison, E. K., Quinlan, A. R., Stromberg, M. P., & Marth, G. T. (2011).
673 BamTools: a C++ API and toolkit for analyzing and managing BAM files. *Bioinformatics*,
674 27(12), 1691–1692. <https://doi.org/10.1093/bioinformatics/btr174>
- 675 Benestan, L. (2019). Population genomics applied to fishery management and conservation.
676 In M. Oleksiak & O. Rajora (Eds.), *Population Genomics: Marine Organisms* (pp. 399–
677 421). Springer. https://doi.org/10.1007/13836_2019_66

- 678 Bernatchez, L., Wellenreuther, M., Araneda, C., Ashton, D. T., Barth, J. M. I., Beacham, T. D.,
679 Maes, G. E., Martinsohn, J. T., Miller, K. M., Naish, K. A., Ovenden, J. R., Primmer, C. R.,
680 Young Suk, H., Therkildsen, N. O., & Withler, R. E. (2017). Harnessing the power of
681 genomics to secure the future of seafood. *Trends in Ecology & Evolution*, 32(9), 665–680.
682 <https://doi.org/10.1016/j.tree.2017.06.010>
- 683 Braunschweig, U., Barbosa-Morais, N. L., Pan, Q., Nachman, E. N., Alipanahi, B.,
684 Gonatopoulos-Pournatzis, T., Frey, B., Irimia, M., & Blencowe, B. J. (2014). Widespread
685 intron retention in mammals functionally tunes transcriptomes. *Genome Research*,
686 24(11), 1774–1786. <https://doi.org/10.1101/gr.177790.114>
- 687 Broad Institute. (2019). *Picard toolkit*. Broad Institute, GitHub Repository.
688 <http://broadinstitute.github.io/picard/>
- 689 Burrows, M. T., Schoeman, D. S., Buckley, L. B., Moore, P., Poloczanska, E. S., Brander, K. M.,
690 Brown, C., Bruno, J. F., Duarte, C. M., Halpern, B. S., Holding, J., Kappel, C. V, Kiessling,
691 W., O'Connor, M. I., Pandolfi, J. M., Parmesan, C., Schwing, F. B., Sydeman, W. J., &
692 Richardson, A. J. (2011). The pace of shifting climate in marine and terrestrial
693 ecosystems. *Science*, 334(6056), 652–655. <https://doi.org/10.1126/science.1210288>
- 694 Bushnell, B. (2018). *BBMap short read aligner*. Berkeley: University of California.
695 <http://sourceforge.net/projects/bbmap>
- 696 Byrne, A., Cole, C., Volden, R., & Vollmers, C. (2019). Realizing the potential of full-length
697 transcriptome sequencing. *Philosophical Transactions of the Royal Society B: Biological*
698 *Sciences*, 374(1786), 20190097. <https://doi.org/10.1098/rstb.2019.0097>
- 699 Camacho, C., Coulouris, G., Avagyan, V., Ma, N., Papadopoulos, J., Bealer, K., & Madden, T. L.
700 (2009). BLAST+: architecture and applications. *BMC Bioinformatics*, 10(1), 1–9.
701 <https://doi.org/10.1186/1471-2105-10-421>
- 702 Challis, R. (2017). *rjchallis/assembly-stats* 17.02. Zenodo.
703 <https://doi.org/https://doi.org/10.5281/zenodo.322347>
- 704 Chen, Y., Wan, S., Li, Q., Dong, X., Diao, J., Liao, Q., Wang, G.-Y., & Gao, Z.-X. (2021). Genome-

- 705 Wide Integrated Analysis revealed functions of lncRNA–miRNA–mRNA interaction in
706 growth of intermuscular bones in *Megalobrama amblycephala*. *Frontiers in Cell and*
707 *Developmental Biology*, 8(603815), 1–15. <https://doi.org/10.3389/fcell.2020.603815>
- 708 Cheng, H., Concepcion, G. T., Feng, X., Zhang, H., & Li, H. (2021). Haplotype-resolved de novo
709 assembly using phased assembly graphs with hifiasm. *Nature Methods*, 18(2), 170–175.
710 <https://doi.org/10.1038/s41592-020-01056-5>
- 711 Dainat, J. (2021). *AGAT: Another Gff Analysis Toolkit to handle annotations in any GTF/GFF*
712 *format*. (Version v0.6.0). Zenodo.
713 <https://doi.org/https://www.doi.org/10.5281/zenodo.3552717>
- 714 Danecek, P., Auton, A., Abecasis, G., Albers, C. A., Banks, E., DePristo, M. A., Handsaker, R. E.,
715 Lunter, G., Marth, G. T., Sherry, S. T., McVean, G., & Durbin, R. (2011). The variant call
716 format and VCFtools. *Bioinformatics*, 27(15), 2156–2158.
717 <https://doi.org/10.1093/bioinformatics/btr330>
- 718 De Coster, W. (2017). *Per base sequence content and quality (new basecaller)*.
719 [https://gigabaseorgigabyte.wordpress.com/2017/05/10/per-base-sequence-content-](https://gigabaseorgigabyte.wordpress.com/2017/05/10/per-base-sequence-content-and-quality-new-basecaller/)
720 [and-quality-new-basecaller/](https://gigabaseorgigabyte.wordpress.com/2017/05/10/per-base-sequence-content-and-quality-new-basecaller/)
- 721 De Coster, W., D’Hert, S., Schultz, D. T., Cruts, M., & Van Broeckhoven, C. (2018). NanoPack:
722 visualizing and processing long-read sequencing data. *Bioinformatics*, 34(15), 2666–
723 2669. <https://doi.org/10.1093/bioinformatics/bty149>
- 724 Dhar, R., Seethy, A., Pethusamy, K., Singh, S., Rohil, V., Purkayastha, K., Mukherjee, I.,
725 Goswami, S., Singh, R., Raj, A., Srivastava, T., Acharya, S., Rajashekhar, B., & Karmakar, S.
726 (2019). De novo assembly of the Indian blue peacock (*Pavo cristatus*) genome using
727 Oxford Nanopore technology and Illumina sequencing. *GigaScience*, 8(5), 1–13.
728 <https://doi.org/10.1093/gigascience/giz038>
- 729 Eddy, S. R. (2011). Accelerated Profile HMM Searches. *PLoS Computational Biology*, 7(10),
730 e1002195. <https://doi.org/10.1371/journal.pcbi.1002195>
- 731 Fan, G., Song, Y., Yang, L., Huang, X., Zhang, S., Zhang, M., Yang, X., Chang, Y., Zhang, H., Li, Y.,

- 732 Liu, S., Yu, L., Chu, J., Seim, I., Feng, C., Near, T. J., Wing, R. A., Wang, W., Wang, K., ... He,
733 S. (2020). Initial data release and announcement of the 10,000 Fish Genomes Project
734 (Fish10K). *GigaScience*, 9(8), 1–7. <https://doi.org/10.1093/gigascience/giaa080>
- 735 Feron, R., Zahm, M., Cabau, C., Klopp, C., Roques, C., Bouchez, O., Eché, C., Valière, S.,
736 Donnadieu, C., Haffray, P., Bestin, A., Morvezen, R., Acloque, H., Euclide, P. T., Wen, M.,
737 Jouano, E., Scharl, M., Postlethwait, J. H., Schraidt, C., ... Guiguen, Y. (2020).
738 Characterization of a Y-specific duplication/insertion of the anti-Mullerian hormone type
739 II receptor gene based on a chromosome-scale genome assembly of yellow perch, *Perca*
740 *flavescens*. *Molecular Ecology Resources*, 20(2), 531–543. [https://doi.org/10.1111/1755-](https://doi.org/10.1111/1755-0998.13133)
741 [0998.13133](https://doi.org/10.1111/1755-0998.13133)
- 742 Fisheries New Zealand. (2018). *Fisheries Assessment Plenary: Stock Assessment and Stock*
743 *Status Volume 3: Pipi to Yellow-eyed Mullet*. Ministry for Primary Industries.
- 744 Flynn, J. M., Hubley, R., Goubert, C., Rosen, J., Clark, A. G., Feschotte, C., & Smit, A. F. (2020).
745 RepeatModeler2 for automated genomic discovery of transposable element families.
746 *Proceedings of the National Academy of Sciences*, 117(17), 9451–9457.
747 <https://doi.org/10.1073/pnas.1921046117>
- 748 Gan, W., Chung-Davidson, Y. W., Chen, Z., Song, S., Cui, W., He, W., Zhang, Q., Li, W., Li, M., &
749 Ren, J. (2021). Global tissue transcriptomic analysis to improve genome annotation and
750 unravel skin pigmentation in goldfish. *Scientific Reports*, 11(1), 1–14.
751 <https://doi.org/10.1038/s41598-020-80168-6>
- 752 Gao, Q., Xiong, Z., Larsen, R. S., Zhou, L., Zhao, J., Ding, G., Zhao, R., Liu, C., Ran, H., & Zhang,
753 G. (2020). High-quality chromosome-level genome assembly and full-length
754 transcriptome analysis of the pharaoh ant *Monomorium pharaonis*. *GigaScience*, 9(12),
755 1–14. <https://doi.org/10.1093/gigascience/giaa143>
- 756 Gao, Y., Xi, F., Liu, X., Wang, H., Reddy, A. S., & Gu, L. (2019). Single-molecule Real-time (SMRT)
757 Isoform Sequencing (Iso-Seq) in Plants: The status of the bioinformatics tools to unravel
758 the transcriptome complexity. *Current Bioinformatics*, 14(7), 566–573.
- 759 Ge, H., Lin, K., Shen, M., Wu, S., Wang, Y., Zhang, Z., Wang, Z., Zhang, Y., Huang, Z., Zhou, C.,

- 760 Lin, Q., Wu, J., Liu, L., Hu, J., Huang, Z., & Zheng, L. (2019). De novo assembly of a
761 chromosome-level reference genome of red-spotted grouper (*Epinephelus akaara*) using
762 nanopore sequencing and Hi-C. *Molecular Ecology Resources*, 19(6), 1461–1469.
763 <https://doi.org/10.1111/1755-0998.13064>
- 764 Gong, G., Dan, C., Xiao, S., Guo, W., Huang, P., Xiong, Y., Wu, J., He, Y., Zhang, J., Li, X., Chen,
765 N., Gui, J. F., & Mei, J. (2018). Chromosomal-level assembly of yellow catfish genome
766 using third-generation DNA sequencing and Hi-C analysis. *GigaScience*, 7(11), 1–9.
767 <https://doi.org/10.1093/gigascience/giy120>
- 768 Hansen, K. D., Brenner, S. E., & Dudoit, S. (2010). Biases in Illumina transcriptome sequencing
769 caused by random hexamer priming. *Nucleic Acids Research*, 38(12), e131–e131.
770 <https://doi.org/10.1093/nar/gkq224>
- 771 Hardwick, S. A., Joglekar, A., Flicek, P., Frankish, A., & Tilgner, H. U. (2019). Getting the Entire
772 Message: Progress in Isoform Sequencing. *Frontiers in Genetics*, 10(709), 1–10.
773 <https://doi.org/10.3389/fgene.2019.00709>
- 774 Hoang, N. V., & Henry, R. J. (2021). Iso-Seq Long Read Transcriptome Sequencing. In A.
775 Cifuentes (Ed.), *Comprehensive Foodomics* (pp. 486–500). Elsevier.
776 <https://doi.org/10.1016/b978-0-08-100596-5.22729-7>
- 777 Holt, C., & Yandell, M. (2011). MAKER2: an annotation pipeline and genome-database
778 management tool for second-generation genome projects. *BMC Bioinformatics*, 12(491),
779 1–14. <https://doi.org/10.1186/1471-2105-12-491>
- 780 Iwasaki, W., Fukunaga, T., Isagozawa, R., Yamada, K., Maeda, Y., Satoh, T. P., Sado, T.,
781 Mabuchi, K., Takeshima, H., Miya, M., & Nishida, M. (2013). MitoFish and
782 MitoAnnotator: A mitochondrial genome database of fish with an accurate and
783 automatic annotation pipeline. *Molecular Biology and Evolution*, 30(11), 2531–2540.
784 <https://doi.org/10.1093/molbev/mst141>
- 785 Jain, C., Koren, S., Dilthey, A., Phillippy, A. M., & Aluru, S. (2018). A fast adaptive algorithm for
786 computing whole-genome homology maps. *Bioinformatics*, 34(17), i748–i756.
787 <https://doi.org/10.1093/bioinformatics/bty597>

- 788 Jansen, H. J., Liem, M., Jong-Raadsen, S. A., Dufour, S., Weltzien, F. A., Swinkels, W., Koelewijn,
789 A., Palstra, A. P., Pelster, B., Spaik, H. P., Thillart, G. E. V. Den, Dirks, R. P., & Henkel, C.
790 V. (2017). Rapid de novo assembly of the European eel genome from nanopore
791 sequencing reads. *Scientific Reports*, 7(1), 1–13. [https://doi.org/10.1038/s41598-017-](https://doi.org/10.1038/s41598-017-07650-6)
792 07650-6
- 793 Jiang, J. B., Quattrini, A. M., Francis, W. R., Ryan, J. F., Rodríguez, E., & McFadden, C. S. (2019).
794 A hybrid de novo assembly of the sea pansy (*Renilla muelleri*) genome. *GigaScience*, 8(4),
795 1–7. <https://doi.org/10.1093/gigascience/giz026>
- 796 Jones, P., Binns, D., Chang, H.-Y., Fraser, M., Li, W., McAnulla, C., McWilliam, H., Maslen, J.,
797 Mitchell, A., Nuka, G., Pesseat, S., Quinn, A. F., Sangrador-Vegas, A., Scheremetjew, M.,
798 Yong, S.-Y., Lopez, R., & Hunter, S. (2014). InterProScan 5: genome-scale protein function
799 classification. *Bioinformatics*, 30(9), 1236–1240.
800 <https://doi.org/10.1093/bioinformatics/btu031>
- 801 Kadobianskyi, M., Schulze, L., Schuelke, M., & Judkewitz, B. (2019). Hybrid genome assembly
802 and annotation of *Danionella translucida*. *Scientific Data*, 6(156), 1:7.
803 <https://doi.org/10.1038/s41597-019-0161-z>
- 804 Kearse, M., Moir, R., Wilson, A., Stones-Havas, S., Cheung, M., Sturrock, S., Buxton, S., Cooper,
805 A., Markowitz, S., Duran, C., Thierer, T., Ashton, B., Meintjes, P., & Drummond, A. (2012).
806 Geneious Basic: An integrated and extendable desktop software platform for the
807 organization and analysis of sequence data. *Bioinformatics*, 28(12), 1647–1649.
808 <https://doi.org/10.1093/bioinformatics/bts199>
- 809 Keel, B. N., & Snelling, W. M. (2018). Comparison of Burrows-Wheeler transform-based
810 mapping algorithms used in high-throughput whole-genome sequencing: Application to
811 illumina data for livestock genomes 1. *Frontiers in Genetics*, 9(35), 1–6.
812 <https://doi.org/10.3389/fgene.2018.00035>
- 813 Kersey, P. J., Allen, J. E., Armean, I., Boddu, S., Bolt, B. J., Carvalho-Silva, D., Christensen, M.,
814 Davis, P., Falin, L. J., Grabmueller, C., Humphrey, J., Kerhornou, A., Khobova, J.,
815 Aranganathan, N. K., Langridge, N., Lowy, E., McDowall, M. D., Maheswari, U., Nuhn, M.,

- 816 ... Staines, D. M. (2016). Ensembl Genomes 2016: more genomes, more complexity.
817 *Nucleic Acids Research*, 44(D1), D574–D580. <https://doi.org/10.1093/nar/gkv1209>
- 818 Kimura, K., Imamura, H., & Kawai, T. (2018). Comparative morphology and phylogenetic
819 systematics of the families Cheilodactylidae and Latridae (Perciformes: Cirrhitidae), and
820 proposal of a new classification. *Zootaxa*, 4536(1), 1–72.
821 <https://doi.org/10.11646/zootaxa.4536.1.1>
- 822 Koepfli, K. P., Paten, B., O'Brien, S. J., Antunes, A., Belov, K., Bustamante, C., Castoe, T. A.,
823 Clawson, H., Crawford, A. J., Diekhans, M., Distel, D., Durbin, R., Earl, D., Fujita, M. K.,
824 Gamble, T., Georges, A., Gemmell, N., Gilbert, M. T. P., Graves, J. M., ... Ryder, O. (2015).
825 The genome 10K project: A way forward. *Annual Review of Animal Biosciences*, 3, 57–
826 111. <https://doi.org/10.1146/annurev-animal-090414-014900>
- 827 Kolmogorov, M., Yuan, J., Lin, Y., & Pevzner, P. A. (2019). Assembly of long, error-prone reads
828 using repeat graphs. *Nature Biotechnology*, 37(5), 540–546.
829 <https://doi.org/10.1038/s41587-019-0072-8>
- 830 Koren, S., Schatz, M. C., Walenz, B. P., Martin, J., Howard, J. T., Ganapathy, G., Wang, Z., Rasko,
831 D. A., McCombie, W. R., Jarvis, E. D., & Phillippy, A. M. (2012). Hybrid error correction
832 and de novo assembly of single-molecule sequencing reads. *Nature Biotechnology*, 30(7),
833 693–700. <https://doi.org/10.1038/nbt.2280>
- 834 Korf, I. (2004). Gene finding in novel genomes. *BMC Bioinformatics*, 5(59).
835 <https://doi.org/10.1186/1471-2105-5-59>
- 836 Kuo, R. I., Cheng, Y., Zhang, R., Brown, J. W. S., Smith, J., Archibald, A. L., & Burt, D. W. (2020).
837 Illuminating the dark side of the human transcriptome with long read transcript
838 sequencing. *BMC Genomics*, 21(751), 1:22. [https://doi.org/10.1186/s12864-020-07123-](https://doi.org/10.1186/s12864-020-07123-7)
839 7
- 840 Kuo, R. I., Tseng, E., Eory, L., Paton, I. R., Archibald, A. L., & Burt, D. W. (2017). Normalized
841 long read RNA sequencing in chicken reveals transcriptome complexity similar to human.
842 *BMC Genomics*, 18(323), 1–19. <https://doi.org/10.1186/s12864-017-3691-9>

- 843 Langley, A. D. (2018). *Stock assessment of tarakihi off the east coast of mainland New Zealand*
844 [New Zealand Fisheries Assessment Report 2018/05]. Ministry for Primary Industries.
- 845 Li, H. (2011). A statistical framework for SNP calling, mutation discovery, association mapping
846 and population genetical parameter estimation from sequencing data. *Bioinformatics*,
847 27(21), 2987–2993. <https://doi.org/10.1093/bioinformatics/btr509>
- 848 Li, H. (2013). *Aligning sequence reads, clone sequences and assembly contigs with BWA-MEM*.
849 <https://arxiv.org/abs/1303.3997v2>
- 850 Li, H. (2018). Minimap2: pairwise alignment for nucleotide sequences. *Bioinformatics*, 34(18),
851 3094–3100. <https://doi.org/10.1093/bioinformatics/bty191>
- 852 Li, H., & Durbin, R. (2009). Fast and accurate short read alignment with Burrows-Wheeler
853 transform. *Bioinformatics*, 25(14), 1754–1760.
854 <https://doi.org/10.1093/bioinformatics/btp324>
- 855 Li, H., Handsaker, B., Wysoker, A., Fennell, T., Ruan, J., Homer, N., Marth, G., Abecasis, G., &
856 Durbin, R. (2009). The Sequence Alignment/Map format and SAMtools. *Bioinformatics*,
857 25(16), 2078–2079. <https://doi.org/10.1093/bioinformatics/btp352>
- 858 Lu, L., Zhao, J., & Li, C. (2020). High-Quality Genome Assembly and Annotation of the Big-Eye
859 Mandarin Fish (*Siniperca kneri*). *G3: Genes, Genomes, Genetics*, 10(3), 877–880.
860 <https://doi.org/10.1534/g3.119.400930>
- 861 Ludt, W. B., BurrIDGE, C. P., & Chakrabarty, P. (2019). A taxonomic revision of Cheilodactylidae
862 and Latridae (Centrarchiformes: Cirrhitidae) using morphological and genomic
863 characters. *Zootaxa*, 4585(1), 121–141. <https://doi.org/10.11646/zootaxa.4585.1.7>
- 864 Marçais, G., & Kingsford, C. (2011). A fast, lock-free approach for efficient parallel counting of
865 occurrences of *k*-mers. *Bioinformatics*, 27(6), 764–770.
866 <https://doi.org/10.1093/bioinformatics/btr011>
- 867 Miller, J. R., Delcher, A. L., Koren, S., Venter, E., Walenz, B. P., Brownley, A., Johnson, J., Li, K.,
868 Mobarry, C., & Sutton, G. (2008). Aggressive assembly of pyrosequencing reads with
869 mates. *Bioinformatics*, 24(24), 2818–2824.

- 870 <https://doi.org/10.1093/bioinformatics/btn548>
- 871 Nguinkal, J. A., Brunner, R. M., Verleih, M., Rebl, A., de los Ríos-Pérez, L., Schäfer, N., Hadlich,
872 F., Stüeken, M., Wittenburg, D., & Goldammer, T. (2019). The first highly contiguous
873 genome assembly of pikeperch (*Sander lucioperca*), an emerging aquaculture species in
874 Europe. *Genes*, *10*(9), 708. <https://doi.org/10.3390/genes10090708>
- 875 Nudelman, G., Frasca, A., Kent, B., Sadler, K. C., Sealfon, S. C., Walsh, M. J., & Zaslavsky, E.
876 (2018). High resolution annotation of zebrafish transcriptome using long-read
877 sequencing. *Genome Research*, *28*(9), 1415–1425.
878 <https://doi.org/10.1101/gr.223586.117>
- 879 Nurk, S., Walenz, B. P., Rhie, A., Vollger, M. R., Logsdon, G. A., Grothe, R., Miga, K. H., Eichler,
880 E. E., Phillippy, A. M., & Koren, S. (2020). HiCanu: Accurate assembly of segmental
881 duplications, satellites, and allelic variants from high-fidelity long reads. *Genome*
882 *Research*, *30*(9), 1291–1305. <https://doi.org/10.1101/GR.263566.120>
- 883 PacBio. (2020). *SMRT Link v9.0*. <https://www.pacb.com/support/software-downloads/>
- 884 Papa, Y., Halliwell, A. G., Morrison, M. A., Wellenreuther, M., & Ritchie, P. A. (2021).
885 Phylogeographic structure and historical demography of tarakihi (*Nemadactylus*
886 *macropterus*) and king tarakihi (*Nemadactylus* n.sp.) in New Zealand. *New Zealand*
887 *Journal of Marine and Freshwater Research*, 1–25.
888 <https://doi.org/10.1080/00288330.2021.1912119>
- 889 Papa, Y., Oosting, T., Valenza-Troubat, N., Wellenreuther, M., & Ritchie, P. A. (2021). Genetic
890 stock structure of New Zealand fish and the use of genomics in fisheries management:
891 an overview and outlook. *New Zealand Journal of Zoology*, *48*(1), 1–31.
892 <https://doi.org/10.1080/03014223.2020.1788612>
- 893 Piccoli, G. R. (2021). *grpciccoli/assemblies-stats: (Version 1.1.1)*. Zenodo.
894 <https://doi.org/10.5281/zenodo.4703697>
- 895 Pootakham, W., Sonthirod, C., Naktang, C., Nawae, W., Yoocha, T., Kongkachana, W.,
896 Sangsrakru, D., Jomchai, N., Uthoomporn, S., Sheedy, J. R., Buaboocha, J., Mekiyanon, S.,

- 897 & Tangphatsornruang, S. (2020). *De novo* assemblies of *Luffa acutangula* and *Luffa*
898 *cylindrica* genomes reveal an expansion associated with substantial accumulation of
899 transposable elements. *Molecular Ecology Resources*, 1–14.
900 <https://doi.org/10.1111/1755-0998.13240>
- 901 Quinlan, A. R., & Hall, I. M. (2010). BEDTools: a flexible suite of utilities for comparing genomic
902 features. *Bioinformatics*, 26(6), 841–842.
903 <https://doi.org/10.1093/bioinformatics/btq033>
- 904 R Core Team. (2020). *R: A language and environment for statistical computing*. R Foundation
905 for Statistical Computing. <http://www.r-project.org/>
- 906 Ramos, J. E., Pecl, G. T., Moltschaniwskyj, N. A., Semmens, J. M., Souza, C. A., & Strugnell, J.
907 M. (2018). Population genetic signatures of a climate change driven marine range
908 extension. *Scientific Reports*, 8, 1–12. <https://doi.org/10.1038/s41598-018-27351-y>
- 909 Rice, E. S., & Green, R. E. (2019). New approaches for genome assembly and scaffolding.
910 *Annual Review of Animal Biosciences*, 7(1), 17–40. [https://doi.org/10.1146/annurev-](https://doi.org/10.1146/annurev-animal-020518-115344)
911 [animal-020518-115344](https://doi.org/10.1146/annurev-animal-020518-115344)
- 912 Roach, M. J., Schmidt, S. A., & Borneman, A. R. (2018). Purge Haplotigs: allelic contig
913 reassignment for third-gen diploid genome assemblies. *BMC Bioinformatics*, 19(460), 1–
914 10. <https://doi.org/10.1186/s12859-018-2485-7>
- 915 Roberts, C. D., Stewart, A. L., & Struthers, C. D. (2015). *The Fishes of New Zealand* (C. D.
916 Roberts, A. L. Stewart, & C. D. Struthers (eds.)). Te Papa Press.
- 917 RStudio Team. (2020). *RStudio: Integrated development environment for R*. RStudio, PBC.
918 <http://www.rstudio.com/>
- 919 Sanciangco, M. D., Carpenter, K. E., & Betancur-R., R. (2016). Phylogenetic placement of
920 enigmatic percomorph families (Teleostei: Percomorphaceae). *Molecular Phylogenetics*
921 *and Evolution*, 94, 565–576. <https://doi.org/10.1016/j.ympev.2015.10.006>
- 922 Shen, W., Le, S., Li, Y., & Hu, F. (2016). SeqKit: A cross-platform and ultrafast toolkit for
923 FASTA/Q file manipulation. *PLOS ONE*, 11(10), e0163962.

- 924 <https://doi.org/10.1371/journal.pone.0163962>
- 925 Simão, F. A., Waterhouse, R. M., Ioannidis, P., Kriventseva, E. V., & Zdobnov, E. M. (2015).
926 BUSCO: assessing genome assembly and annotation completeness with single-copy
927 orthologs. *Bioinformatics*, 31(19), 3210–3212.
928 <https://doi.org/10.1093/bioinformatics/btv351>
- 929 Simison, W. B., Parham, J. F., Papenfuss, T. J., Lam, A. W., Henderson, J. B., Brian Simison, W.,
930 Parham, J. F., Papenfuss, T. J., Lam, A. W., & Henderson, J. B. (2020). An annotated
931 chromosome-level reference genome of the red-eared slider turtle (*Trachemys scripta*
932 *elegans*). *Genome Biology and Evolution*, 12(4), 456–462.
933 <https://doi.org/10.1093/gbe/evaa063>
- 934 Smit, A., Hubley, R., & Green, P. (2013). *RepeatMasker Open-4.0*.
935 <http://www.repeatmasker.org>
- 936 Stanke, M., Steinkamp, R., Waack, S., & Morgenstern, B. (2004). AUGUSTUS: a web server for
937 gene finding in eukaryotes. *Nucleic Acids Research*, 32(Web Server), W309–W312.
938 <https://doi.org/10.1093/nar/gkh379>
- 939 Storer, J., Hubley, R., Rosen, J., Wheeler, T. J., & Smit, A. F. (2021). The Dfam community
940 resource of transposable element families, sequence models, and genome annotations.
941 *Mobile DNA*, 12(2), 1–14. <https://doi.org/10.1186/s13100-020-00230-y>
- 942 Sun, C., Li, J., Dong, J., Niu, Y., Hu, J., Lian, J., Li, W., Li, J., Tian, Y., Shi, Q., & Ye, X. (2021).
943 Chromosome-level genome assembly for the largemouth bass *Micropterus salmoides*
944 provides insights into adaptation to fresh and brackish water. *Molecular Ecology*
945 *Resources*, 21(1), 301–315. <https://doi.org/10.1111/1755-0998.13256>
- 946 Takehana, Y., Zahm, M., Cabau, C., Klopp, C., Roques, C., Bouchez, O., Donnadieu, C.,
947 Barrachina, C., Journot, L., Kawaguchi, M., Yasumasu, S., Ansai, S., Naruse, K., Inoue, K.,
948 Shinzato, C., Scharl, M., Guiguen, Y., & Herpin, A. (2020). Genome sequence of the
949 euryhaline javafish medaka, *Oryzias javanicus* : A small aquarium fish model for studies
950 on adaptation to salinity. *G3: Genes, Genomes, Genetics*, 10(3), 907–915.
951 <https://doi.org/10.1534/g3.119.400725>

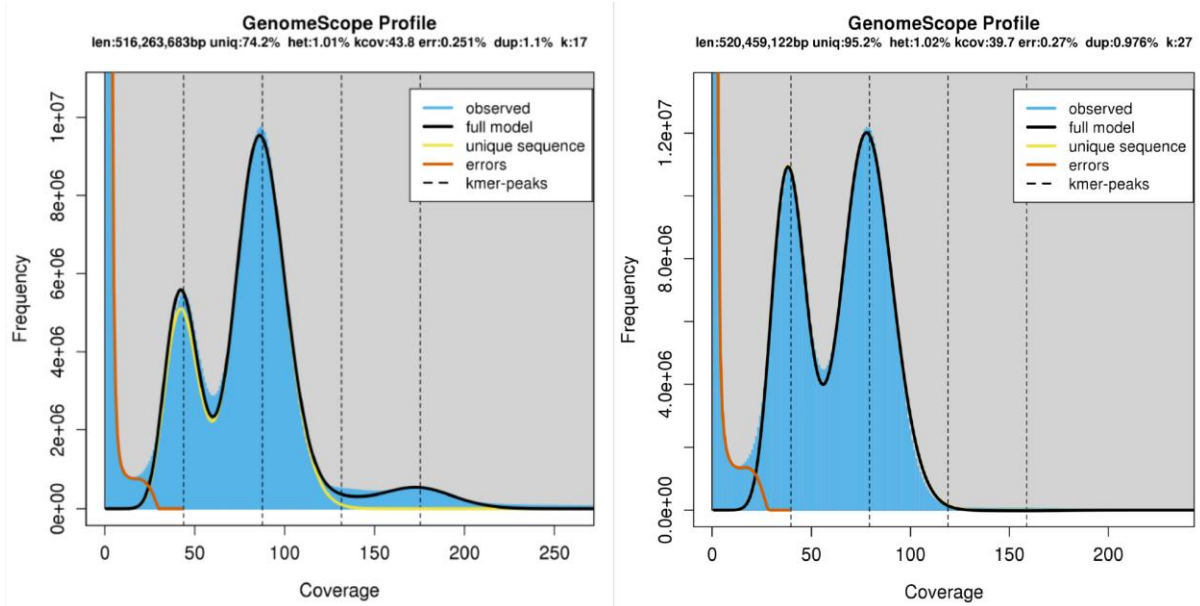
- 952 Tan, M. H., Austin, C. M., Hammer, M. P., Lee, Y. P., Croft, L. J., & Gan, H. M. (2018). Finding
953 Nemo: hybrid assembly with Oxford Nanopore and Illumina reads greatly improves the
954 clownfish (*Amphiprion ocellaris*) genome assembly. *GigaScience*, 7(3), 1–6.
955 <https://doi.org/10.1093/gigascience/gix137>
- 956 Thai, B. T., Lee, Y. P., Gan, H. M., Austin, C. M., Croft, L. J., Trieu, T. A., & Tan, M. H. (2019).
957 Whole genome assembly of the snout otter clam, *Lutraria rhynchaena*, using Nanopore
958 and Illumina data, benchmarked against bivalve genome assemblies. *Frontiers in*
959 *Genetics*, 10(1158), 1–8. <https://doi.org/10.3389/fgene.2019.01158>
- 960 Thomson, A. I., Archer, F. I., Coleman, M. A., Gajardo, G., Goodall-Copestake, W. P., Hoban,
961 S., Laikre, L., Miller, A. D., O'Brien, D., Pérez-Espona, S., Segelbacher, G., Serrão, E. A.,
962 Sjøtun, K., & Stanley, M. S. (2021). Charting a course for genetic diversity in the UN
963 Decade of Ocean Science. *Evolutionary Applications*, November 2020, 1–22.
964 <https://doi.org/10.1111/eva.13224>
- 965 Trincado, J. L., Entizne, J. C., Hysenaj, G., Singh, B., Skalic, M., Elliott, D. J., & Eyras, E. (2018).
966 SUPPA2: Fast, accurate, and uncertainty-aware differential splicing analysis across
967 multiple conditions. *Genome Biology*, 19(1), 1–11. [https://doi.org/10.1186/s13059-018-](https://doi.org/10.1186/s13059-018-1417-1)
968 [1417-1](https://doi.org/10.1186/s13059-018-1417-1)
- 969 Vezzi, F., Narzisi, G., & Mishra, B. (2012a). Reevaluating assembly evaluations with Feature
970 Response Curves: GAGE and assemblathons. *PLoS ONE*, 7(12), e52210.
971 <https://doi.org/10.1371/journal.pone.0052210>
- 972 Vezzi, F., Narzisi, G., & Mishra, B. (2012b). Feature-by-Feature – Evaluating De Novo Sequence
973 Assembly. *PLoS ONE*, 7(2), e31002. <https://doi.org/10.1371/journal.pone.0031002>
- 974 Vij, S., Kuhl, H., Kuznetsova, I. S., Komissarov, A., Yurchenko, A. A., Van Heusden, P., Singh, S.,
975 Thevasagayam, N. M., Prakki, S. R. S., Purushothaman, K., Saju, J. M., Jiang, J., Mbandi,
976 S. K., Jonas, M., Hin Yan Tong, A., Mwangi, S., Lau, D., Ngho, S. Y., Liew, W. C., ... Orbán,
977 L. (2016). Chromosomal-level assembly of the Asian seabass genome using long
978 sequence reads and multi-layered scaffolding. *PLoS Genetics*, 12(4), 1–35.
979 <https://doi.org/10.1371/journal.pgen.1005954>

- 980 Vurture, G. W., Sedlazeck, F. J., Nattestad, M., Underwood, C. J., Fang, H., Gurtowski, J., &
981 Schatz, M. C. (2017). GenomeScope: fast reference-free genome profiling from short
982 reads. *Bioinformatics*, 33(14), 2202–2204.
983 <https://doi.org/10.1093/bioinformatics/btx153>
- 984 Wang, X., You, X., Langer, J. D., Hou, J., Rupprecht, F., Vlatkovic, I., Quedenau, C., Tushev, G.,
985 Epstein, I., Schaefer, B., Sun, W., Fang, L., Li, G., Hu, Y., Schuman, E. M., & Chen, W.
986 (2019). Full-length transcriptome reconstruction reveals a large diversity of RNA and
987 protein isoforms in rat hippocampus. *Nature Communications*, 10(5009), 1–15.
988 <https://doi.org/10.1038/s41467-019-13037-0>
- 989 Wang, Y., Lu, Y., Zhang, Y., Ning, Z., Li, Y., Zhao, Q., Lu, H., Huang, R., Xia, X., Feng, Q., Liang,
990 X., Liu, K., Zhang, L., Lu, T., Huang, T., Fan, D., Weng, Q., Zhu, C., Lu, Y., ... Zhu, Z. (2015).
991 The draft genome of the grass carp (*Ctenopharyngodon idellus*) provides insights into its
992 evolution and vegetarian adaptation. *Nature Genetics*, 47(6), 625–631.
993 <https://doi.org/10.1038/ng.3280>
- 994 Wen, M., Ng, J. H. J., Zhu, F., Chionh, Y. T., Chia, W. N., Mendenhall, I. H., Lee, B. P. Y. H., Irving,
995 A. T., & Wang, L. F. (2018). Exploring the genome and transcriptome of the cave nectar
996 bat *Eonycteris spelaea* with PacBio long-read sequencing. *GigaScience*, 7(10), 1–8.
997 <https://doi.org/10.1093/gigascience/giy116>
- 998 Whibley, A., Kelley, J. L., & Narum, S. R. (2021). The changing face of genome assemblies:
999 Guidance on achieving high-quality reference genomes. *Molecular Ecology Resources*,
1000 21(3), 641–652. <https://doi.org/10.1111/1755-0998.13312>
- 1001 Wiley, G., & Miller, M. J. (2020). A highly contiguous genome for the golden-fronted
1002 woodpecker (*Melanerpes aurifrons*) via hybrid Oxford Nanopore and short read
1003 assembly. *G3: Genes, Genomes, Genetics*, 10(6), 1829–1836.
1004 <https://doi.org/10.1534/g3.120.401059>
- 1005 Wood, D. E. (2019). *MiniKraken2 v2 8GB database*. Johns Hopkins University.
1006 ftp://ftp.ccb.jhu.edu/pub/data/kraken2_dbs/old/minikraken2_v2_8GB_201904.tgz
- 1007 Wood, D. E., Lu, J., & Langmead, B. (2019). Improved metagenomic analysis with Kraken 2.

- 1008 *Genome Biology*, 20(257), 1–13. <https://doi.org/10.1186/s13059-019-1891-0>
- 1009 Worley, K. C., Richards, S., & Rogers, J. (2017). The value of new genome references.
1010 *Experimental Cell Research*, 358(2), 433–438.
1011 <https://doi.org/10.1016/j.yexcr.2016.12.014>
- 1012 Wu, C., Zhang, D., Kan, M., Lv, Z., Zhu, A., Su, Y., Zhou, D., Zhang, J., Zhang, Z., Xu, M., Jiang,
1013 L., Guo, B., Wang, T., Chi, C., Mao, Y., Zhou, J., Yu, X., Wang, H., Weng, X., ... Liu, Y. (2014).
1014 The draft genome of the large yellow croaker reveals well-developed innate immunity.
1015 *Nature Communications*, 5(5227), 1–7. <https://doi.org/10.1038/ncomms6227>
- 1016 Yang, X., Liu, H., Ma, Z., Zou, Y., Zou, M., Mao, Y., Li, X., Wang, H., Chen, T., Wang, W., & Yang,
1017 R. (2019). Chromosome-level genome assembly of *Triplophysa tibetana*, a fish adapted
1018 to the harsh high-altitude environment of the Tibetan Plateau. *Molecular Ecology*
1019 *Resources*, 19(4), 1027–1036. <https://doi.org/10.1111/1755-0998.13021>
- 1020 Yuan, Z., Liu, S., Zhou, T., Tian, C., Bao, L., Dunham, R., & Liu, Z. (2018). Comparative genome
1021 analysis of 52 fish species suggests differential associations of repetitive elements with
1022 their living aquatic environments. *BMC Genomics*, 19(141), 1–10.
1023 <https://doi.org/10.1186/s12864-018-4516-1>
- 1024 Zhang, H. H., Xu, M. R. X., Wang, P. L., Zhu, Z. G., Nie, C. F., Xiong, X. M., Wang, L., Xie, Z. Z.,
1025 Wen, X., Zeng, Q. X., Zhang, X. G., & Dai, F. Y. (2020). High-quality genome assembly and
1026 transcriptome of *Ancherythroculter nigrocauda*, an endemic Chinese cyprinid species.
1027 *Molecular Ecology Resources*, 20(4), 882–891. [https://doi.org/10.1111/1755-](https://doi.org/10.1111/1755-0998.13158)
1028 [0998.13158](https://doi.org/10.1111/1755-0998.13158)
- 1029 Zhang, X., Li, G., Jiang, H., Li, L., Ma, J., Li, H., & Chen, J. (2019). Full-length transcriptome
1030 analysis of *Litopenaeus vannamei* reveals transcript variants involved in the innate
1031 immune system. *Fish & Shellfish Immunology*, 87, 346–359.
1032 <https://doi.org/10.1016/j.fsi.2019.01.023>
- 1033 Zheng, S., Shao, F., Tao, W., Liu, Z., Long, J., Wang, X., Zhang, S., Zhao, Q., Carleton, K. L.,
1034 Kocher, T. D., Jin, L., Wang, Z., Peng, Z., Wang, D., & Zhang, Y. (2021). Chromosome-level
1035 assembly of Southern catfish (*Silurus meridionalis*) provides insights into visual

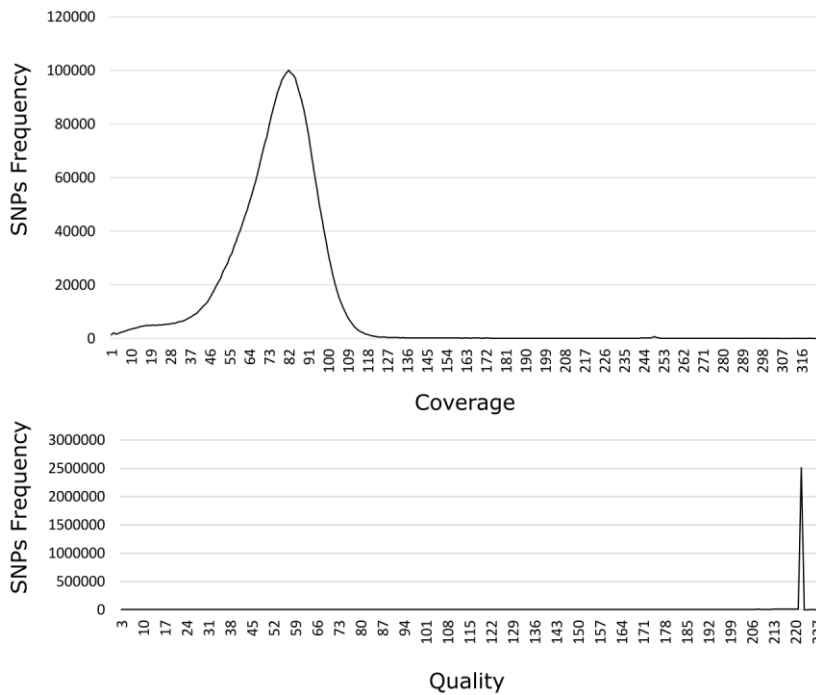
- 1036 adaptation to the nocturnal and benthic lifestyles. *Molecular Ecology Resources*.
1037 <https://doi.org/10.1111/1755-0998.13338>
- 1038 Zimin, A. V., Marçais, G., Puiu, D., Roberts, M., Salzberg, S. L., & Yorke, J. A. (2013). The
1039 MaSuRCA genome assembler. *Bioinformatics*, 29(21), 2669–2677.
1040 <https://doi.org/10.1093/bioinformatics/btt476>
- 1041 Zimin, A. V., Puiu, D., Luo, M.-C., Zhu, T., Koren, S., Marçais, G., Yorke, J. A., Dvořák, J., &
1042 Salzberg, S. L. (2017). Hybrid assembly of the large and highly repetitive genome of
1043 *Aegilops tauschii*, a progenitor of bread wheat, with the MaSuRCA mega-reads
1044 algorithm. *Genome Research*, 27(5), 787–792. <https://doi.org/10.1101/gr.213405.116>
- 1045 Zimin, A. V., & Salzberg, S. L. (2020). The genome polishing tool POLCA makes fast and
1046 accurate corrections in genome assemblies. *PLoS Computational Biology*, 16(6), 1–8.
1047 <https://doi.org/10.1371/journal.pcbi.1007981>
- 1048 Zimin, A. V., Stevens, K. A., Crepeau, M. W., Puiu, D., Wegrzyn, J. L., Yorke, J. A., Langley, C. H.,
1049 Neale, D. B., & Salzberg, S. L. (2017). An improved assembly of the loblolly pine mega-
1050 genome using long-read single-molecule sequencing. *GigaScience*, 6(1), 1–4.
1051 <https://doi.org/10.1093/gigascience/giw016>
- 1052

1053 **11. Supplementary Material**



1054

1055 Supplementary Figure 1. Histograms of 17- and 27-mer frequency in clean Illumina reads.



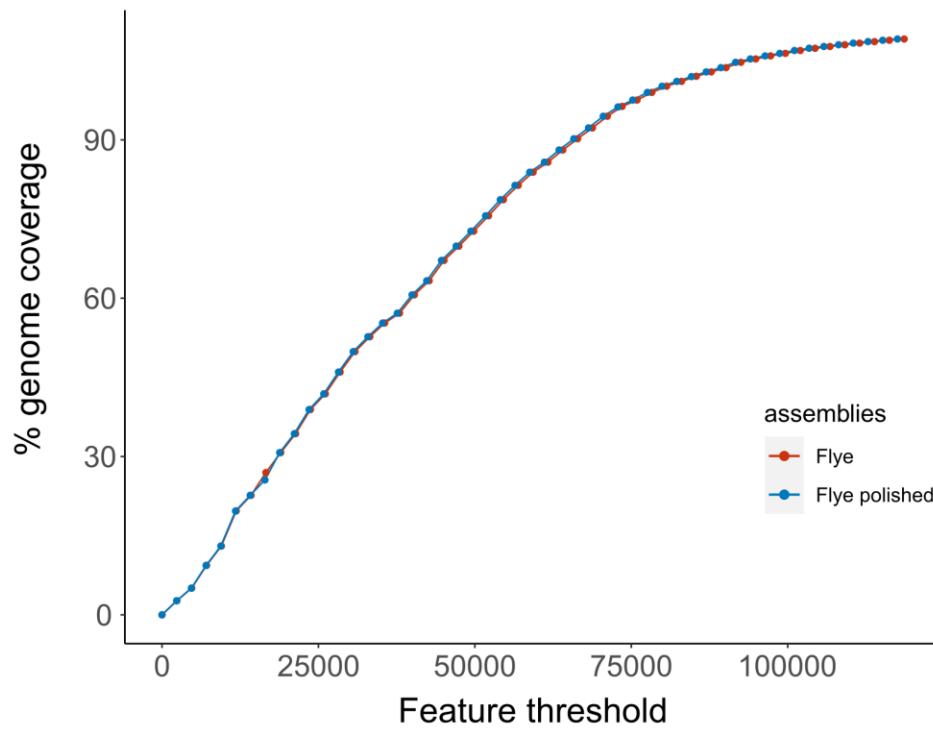
1056

1057 Supplementary Figure 2. Distribution of coverage (top) and quality (bottom) of SNPs called
1058 from Illumina reads back to the assembly. SNPs were filtered for a minimum genotype depth
1059 of 20 according to the increase in steepness starting approximately at this point. Quality was
1060 always high, so the default site quality value was used.



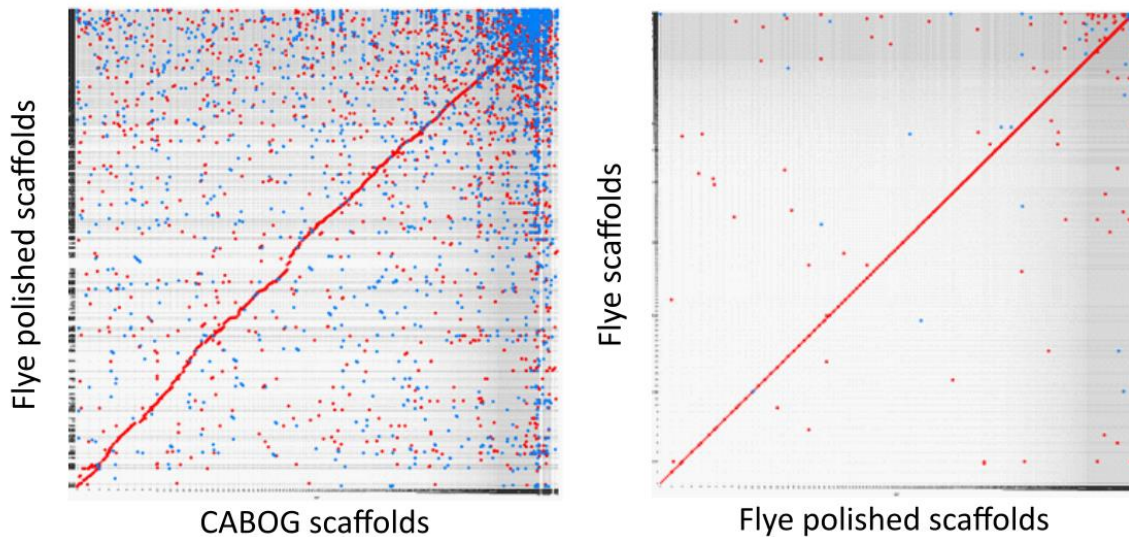
1061

1062 Supplementary Figure 3. Some of FastQC quality metrics results, for forward (R1) and reverse
1063 (R2) reads. Top: Per base sequence quality. Middle: Per base sequence base content. Bottom:
1064 GC distribution over all sequences. See main text for the explanation on the slight bias in
1065 bases content for the first few bases in all reads. GC content of reverse reads detected a few
1066 over-represented sequences, which were most probably harmless sequencing artifacts that
1067 should be discarded during the quality control step of the MaSuRCA assembly.



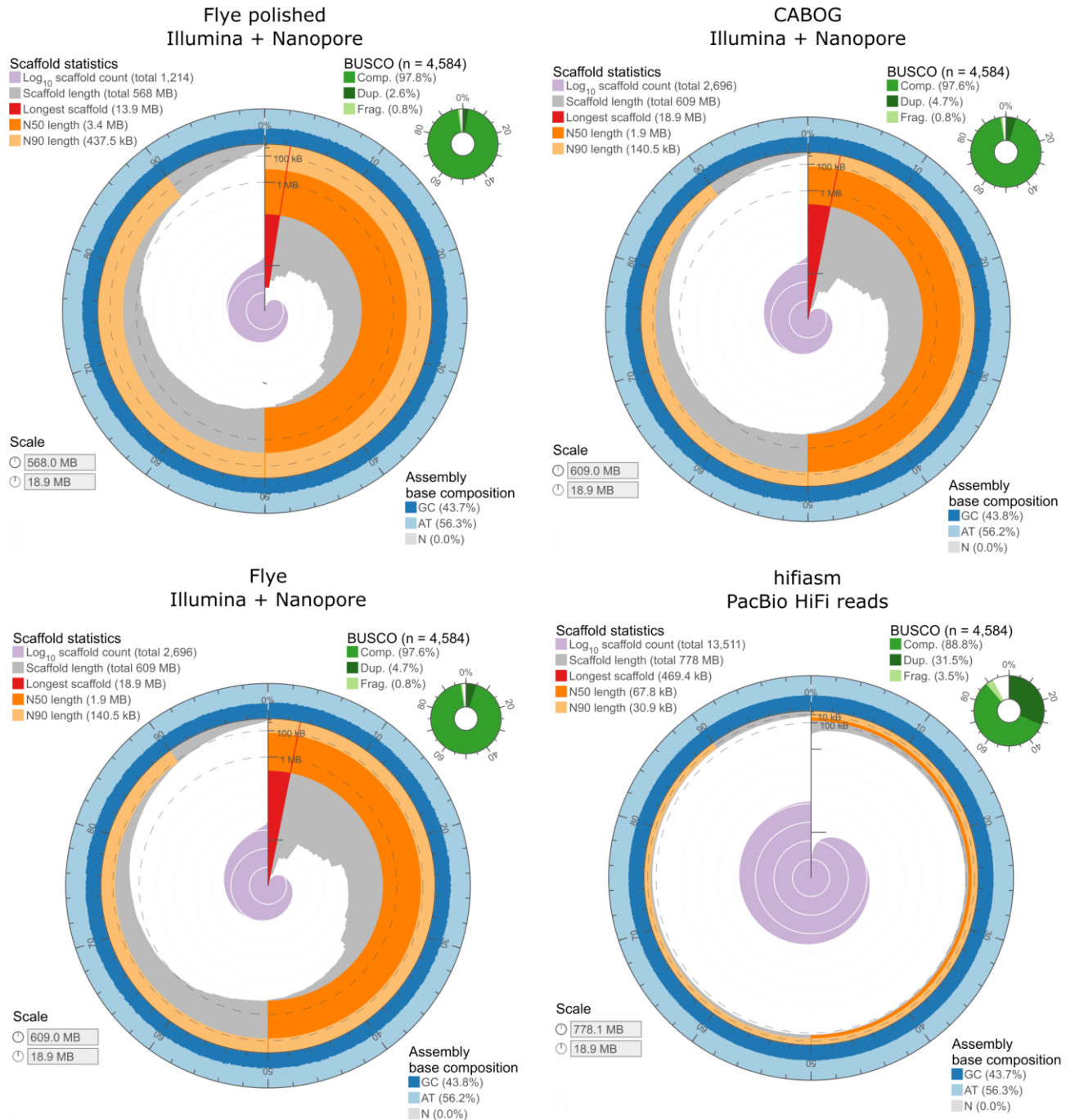
1068

1069 Supplementary Figure 4. FRC curves as shown in Figure 3, but with only the Flye and Flye
1070 polished assemblies projected for better visualization. For the same cumulative genome size,
1071 the Flye unpolished assembly always accumulates slightly more potential errors (i.e.
1072 features).



1073

1074 Supplementary Figure 5. Plots of pairwise alignment scores between scaffolds, obtained with
1075 MashMap. Each dot represents a match between the query and the reference sequence.
1076 Colors correspond to the strand direction (red for positive, blue for negative).



1077

1078 Supplementary Figure 6. Visualization of contiguity and completeness of the four assemblies

1079 produced.

1080 Supplementary Table 1. Main classes and proportions of repeat elements detected in the
1081 tarakihi genome.

Repeat type	No. of elements	Length occupied (bp)	% in the genome
Retroelements	323634	35060271	6.17
SINEs	33606	2627490	0.46
Penelope	8128	793327	0.14
LINEs	214886	24389420	4.29
CRE/SLACS	1	69	0
L2/CR1/Rex	139371	15942708	2.81
R1/LOA/Jockey	6466	805273	0.14
R2/R4/NeSL	5543	659291	0.12
RTE/Bov-B	24021	2686662	0.47
L1/CIN4	12218	1572014	0.28
LTR elements	75142	8043361	1.42
BEL/Pao	6293	705505	0.12
Ty1/Copia	3175	392807	0.07
Gypsy/DIRS1	36293	4302376	0.76
Retroviral	15032	1103666	0.19
DNA transposons	578638	61749831	10.87
hobo-Activator	293706	32369155	5.7
Tc1-IS630-Pogo	80564	7567833	1.33
En-Spm	0	0	0
MuDR-IS905	0	0	0
PiggyBac	13600	1089280	0.19
Tourist/Harbinger	44201	5208743	0.92
Other	11367	1081984	0.19
Rolling-circles	35706	2925989	0.52
Unclassified	458433	60021928	10.57
Total interspersed repeats		156832030	27.62
Small RNA	9364	715919	0.13
Satellites	6240	816959	0.14
Simple repeats	238583	10392751	1.83
Low complexity	28658	1630008	0.29

1082

1083 Supplementary Table 2. Quality control statistics of the gene models obtained after different
1084 rounds of MAKER.

	Round 1	Round 2	Round 3
Number of gene models	9,008	20,327	19,930
Average gene length	11,455	13,741	14,057
AED \leq 0.5	100%	95.50%	94.00%
Complete BUSCO transcripts	58.70%	76.00%	74.90%

1085